### Title

Regulation of Telomere Length Requires a Conserved N-Terminal Domain of Rif2 in Saccharomyces cerevisiae




### Journal

Genetics, 201(2)

### ISSN

0016-6731



### Authors

Kaizer, Hannah
Connelly, Carla J
Bettridge, Kelsey
et al.



### Publication Date

2015-10-01

### DOI

10.1534/genetics.115.177899

Peer reviewed

# Regulation of Telomere Length Requires a Conserved N-Terminal Domain of Rif2 in *Saccharomyces cerevisiae*

**Hannah Kaizer,[1] Carla J. Connelly,[1] Kelsey Bettridge,[2] Christopher Viggiani,[3] and Carol W. Greider[4]**
Department of Molecular Biology and Genetics, Johns Hopkins University School of Medicine, Baltimore, Maryland 21205
ORCID ID: 0000-0002-5494-8126 (C.W.G.)

**ABSTRACT** The regulation of telomere length equilibrium is essential for cell growth and survival since critically short telomeres signal DNA damage and cell cycle arrest. While the broad principles of length regulation are well established, the molecular mechanism of how these steps occur is not fully understood. We mutagenized the *RIF2* gene in *Saccharomyces cerevisiae* to understand how this protein blocks excess telomere elongation. We identified an N-terminal domain in Rif2 that is essential for length regulation, which we have termed BAT domain for **B**locks **A**ddition of **T**elomeres. Tethering this BAT domain to Rap1 blocked telomere elongation not only in *rif2Δ* mutants but also in *rif1Δ* and *rap1C-terminal* deletion mutants. Mutation of a single amino acid in the BAT domain, phenylalanine at position 8 to alanine, recapitulated the *rif2Δ* mutant phenotype. Substitution of F8 with tryptophan mimicked the wild-type phenylalanine, suggesting the aromatic amino acid represents a protein interaction site that is essential for telomere length regulation.

**KEYWORDS** telomeres; telomerase; Rif2; length regulation

THE establishment and maintenance of telomere length equilibrium is essential for cell survival. Yeast cells that fail to maintain telomeres undergo senescence (Lundblad and Szostak 1989), which is mediated by the DNA damage response to short telomeres (Enomoto *et al.* 2002; Ijpma and Greider 2003). In primary human cell cultures, short telomeres initiate replicative senescence (Harley *et al.* 1990; Bodnar *et al.* 1998) by signaling DNA damage (D'Adda di Fagagna *et al.* 2003). This cellular response to short telomeres underlies a spectrum of human diseases that includes bone marrow failure, pulmonary fibrosis, and immune senescence, collectively called the telomere syndromes (Armanios and Blackburn 2012). Conversely, inappropriate telomere maintenance allows the survival of cancer cells (Kim *et al.* 1994), and mutations that increase telomerase expression predispose people to melanoma (Horn *et al.* 2013; Huang *et al.* 2013) and other cancers (Heidenreich *et al.* 2014). To fully address the role of telomeres in disease, a detailed mechanistic understanding of telomere length maintenance is critical.

Telomere sequence DNA repeats are bound by a set of proteins that mediate two essential functions: first, to protect the ends from degradation, recombination, and initiation of a damage response and second, to regulate telomere elongation by telomerase. Telomerase adds telomere repeats to chromosome ends to counterbalance the shortening that occurs during replication (Greider and Blackburn 1985), but this addition must be regulated. While the telomere-binding proteins in *Saccharomyces cerevisiae* and mammalian cells are not conserved in sequence, the function of telomere binding proteins limiting telomere elongation is conserved across eukaryotes (Smogorzewska and de Lange 2004). In yeast, deletion of the genes encoding the telomere binding proteins Rif1 and Rif2 leads to telomere elongation (Hardy *et al.* 1992; Wotton and Shore 1997). In mammals, removal of telomere binding proteins from the telomere, including TRF1, TRF2,


doi: 10.1534/genetics.115.177899
Manuscript received May 4, 2015; accepted for publication August 19, 2015; published Early Online August 20, 2015.
Available freely online through the author-supported open access option.
Supporting information is available online at www.genetics.org/lookup/suppl/doi:10.1534/genetics.115.177899/-/DC1.
[1]These authors contributed equally to this work.
[2]Present address: Program in Molecular Biophysics, Johns Hopkins University School of Medicine, Baltimore, MD 21205.
[3]Present address: National Institutes of Health, Office of Science Policy, Bethesda, MD 20817.
[4]Corresponding author: Department of Molecular Biology and Genetics, Johns Hopkins University School of Medicine, 603 Pre-Clinical Teaching Bldg., 725 N. Wolfe St., Baltimore, MD 21205. E-mail: cgreider@jhmi.edu

and POT1, also results in telomere elongation (van Steensel and de Lange 1997; Smith and de Lange 2000; Colgin *et al.* 2003; Veldman *et al.* 2004; Palm and de Lange 2008). The conservation of this negative length regulation pathway highlights the importance of understanding the mechanism that limits telomere elongation.

In yeast, the Rap1/Rif1/Rif2 protein complex binds to the double-stranded telomere repeats (Longtine *et al.* 1989; Hardy *et al.* 1992; Wotton and Shore 1997), and the Cdc13 complex (Lin and Zakian 1996; Nugent *et al.* 1996) binds to the single-stranded G-rich 3′ overhang. Cdc13 interacts with Stn1 and Ten1 (Grandin *et al.* 1997, 2001) to form a RPA (Replication Protein A)-like trimeric complex (Gao *et al.* 2007) that regulates telomere elongation. In addition to these DNA binding complexes, there are other proteins that associate with telomeres and help regulate both end protection and telomere length. These include a number of proteins that are involved in DNA break repair and checkpoint signaling, such as the MRX (Mre11, Rad50, Xrs2) complex, the Ku70/80 heterodimer, and the Tel1/ATM protein kinase (Shore and Bianchi 2009; Wellinger and Zakian 2012).

In yeast, Rap1 recruits the Rif1 and Rif2 proteins that limit telomere elongation (Hardy *et al.* 1992; Marcand *et al.* 1997; Wotton and Shore 1997; Levy and Blackburn 2004). Deletion of either *RIF1* or *RIF2* results in long telomeres and deletion of the two together has an additive effect, resulting in very long telomeres. Rif1 and Rif2 bind to the C-terminal domain of Rap1, and deletion of this domain results in very long telomeres, similar to the *rif1Δ rif2Δ* double mutant (Wotton and Shore 1997). This additive effect suggests these two proteins might use different mechanisms to limit telomere elongation.

A protein-counting model for negative regulation of telomere elongation was first proposed in yeast (Marcand *et al.* 1997). This model suggests the more Rap1/Rif1/Rif2 complexes that are bound along the telomere, the larger the repressive effect of telomere elongation. Thus, short telomeres have fewer repressive proteins bound and are more frequently elongated, whereas on longer telomeres, the Rap1/Rif1/Rif2 exerts a strong repressive effect so these telomeres are elongated less frequently. Recruiting Rif1 and Rif2 to the telomere by fusion to other DNA binding domains also limits telomere elongation, indicating it is Rif1 and Rif2 function, rather than Rap1 *per se*, that limits telomere elongation (Levy and Blackburn 2004). The interplay of the preferential elongation of short telomeres (Bianchi and Shore 2008) and limiting the extent of elongation at long telomeres is thought to mediate the telomere length equilibrium.

The molecular mechanism by which Rif1 and Rif2 limit telomere elongation remains unclear. In mammalian cells, Rif1 was shown to play a role in replication fork progression (Buonomo *et al.* 2009) and in the timing of replication origin firing (Cornacchia *et al.* 2012; Yamazaki *et al.* 2012). This role in regulating origin firing is conserved in yeast (Lian *et al.* 2011; Mattarocci *et al.* 2014; Peace *et al.* 2014) where Rif1 also functions in regulating resection of double-strand breaks and DNA recombination (Di Virgilio *et al.* 2013; Escribano-Diaz *et al.* 2013; Zimmermann *et al.* 2013).

Like *RIF1*, the *RIF2* gene in yeast also plays a role in protecting chromosome ends from resection. *rif2Δ* mutants show increased single-stranded DNA at telomeres (Bonetti *et al.* 2010a) that requires the MRX complex and its regulator, the Tel1 kinase (Bonetti *et al.* 2010b). Moreover, *in vitro* experiments have suggested that Rif2 binds directly to the C-terminal region of Xrs2 and regulates telomere length through the Tel1 pathway (Hirano *et al.* 2009). Rif2 also protects telomeres from chromosome fusion events (DuBois *et al.* 2002), and the increased rate of senescence of telomerase mutants in the absence of *RIF2* further supports a role for Rif2 in end protection (Chang *et al.* 2011; Ballew and Lundblad 2013; Hu *et al.* 2013). Whether this end-protection role of Rif2 is related to the telomere elongation phenotype of the *rif2Δ* is not known.

The Rif2 protein structure was recently determined both alone and in complex with the C-terminal region of Rap1 (Shi *et al.* 2013). This structure revealed two different areas of contact between Rif2 and Rap1. The authors propose a Velcro model of interlocking protein interactions between Rap1, Rif1, and Rif2, which generate a chromatin scaffold that limits telomere elongation.

To more clearly define the molecular functions of Rif2, we carried out a mutagenesis screen across the entire *RIF2* coding region. We describe here the identification of a domain in the N terminus that blocks telomere elongation by telomerase. Furthermore, mutation of a single amino acid in this domain mimics telomere lengthening seen in *rif2Δ*, suggesting that it is a critical residue for *RIF2* function.

## Materials and Methods

### *Construction of plasmids and yeast strains*

All of the *S. cerevisiae* strains (termed "yeast strains") and oligonucleotides (termed "primers") for polymerase chain reaction (PCR) and for construction of plasmids used in this study are listed in Supporting Information, Table S1, Table S2, Table S3, Table S4, Table S5, and Table S6. All restriction enzymes used in these experiments were from New England Biolabs.

### *NAAIRS mutagenesis*

We scanned the entire *RIF2* gene substituting every six codons with the sequence specifying the amino acid sequence asparagine-alanine-alanine-isoleucine-arginine-serine (NAAIRS) in continuous blocks. *RIF2* was amplified from yeast genomic DNA using primers Rif2-up and Rif2-down by PCR and the 1.67-kb product was subcloned into pCR2.1-TOPO (Life Technologies) according to the manufacturer's instructions. *RIF2* was then subcloned into pRS406 (Sikorski and Hieter 1989) using *Kpn*I and *Eco*RI. This plasmid was used to generate 66 *rif2NAAIRS* mutants using a three-step PCR strategy (Mosher *et al.* 2006). Using the construction of NAAIRS2 as an example, the first PCR incorporated the sequence

encoding the NAAIRS amino acids at positions 2–7 by amplifying the 5′ end of *RIF2* using NAAIRS2 reverse primer, Rif2 forward primer, and the template p406-Rif2. In the second PCR, the anti-NAAIRS2 forward primer, Rif2 reverse primer, and the template p406-Rif2 were used to amplify the remaining 3′ end of *RIF2*, also incorporating the NAAIRS substitution at amino acids 2–7. The PCR products from reactions 1 and 2 were diluted 1:100 and used as templates for amplification in a third PCR using Rif2 forward primer and Rif2 reverse primer. This generated a full-length *rif2–NAAIRS2* product that was subcloned into pCR2.1-TOPO and then inserted into pRS406 using *Kpn*I and *Eco*RI to generate pNAAIRS2. Using this approach, 66 plasmids with the NAAIRS amino acid sequences substituted for continuous blocks of six amino acids within *RIF2* were constructed. All plasmids were confirmed by sequencing and are available upon request.

### Integration of the RIF2–NAAIRS mutants at the URA3 locus

The parental diploid strain for the *rif2* mutagenesis was derived from W303-1a and W303-1α strains provided by O. Aparicio (OAy1002, OAy1003) (Viggiani and Aparicio 2006). *RIF2* was deleted by PCR-based methods as described (Brachmann *et al.* 1998). Yeast strains containing the *RIF2–NAAIRS* mutations were constructed by transforming a *RIF2/rif2Δ*::*kanMX4* diploid (CVy245) with the NAAIRS mutant plasmids cut with *Nco*I within the plasmid-borne *URA3*, which directs integration of the plasmid into the *ura3-1* locus. Transformants were selected for Ura$^+$. Proper integration into the yeast chromosome was confirmed by PCR. The resulting *RIF2/rif2Δ*::*kanMX4*, *ura3-1/ura3-1*::*(rif2NAAIRS-URA3)* strains were sporulated, dissected, and haploids of the desired genotype were grown for Southern blot analysis of telomere length. Following telomere length analysis the *rif2NAAIRS* integrant was PCR amplified from genomic DNA and sequenced to reconfirm the expected NAAIRS mutation. *RIF2* was integrated at the *URA3* locus to generate the wild-type control strain. Yeast culture conditions, transformations, and dissections were performed as described (Green and Sambrook 2012).

### Epitope-tagged RIF2

We used two different epitope tags to determine the expression level of *RIF2* mutants by Western analysis. We used a 13xMyc epitope to tag the NAAIRS mutants at the *URA3* locus and actin as a loading control. For the single amino acid mutants integrated at the *RIF2* locus, we used a V5 epitope tag and phosphoglycerol kinase (PGK) as a loading control. We tagged *RIF2* and specific *rif2–NAAIRS* mutants integrated at the *URA3* locus by a one-step PCR-based method using pFA6a-13xMyc-*His3MX6* (Longtine *et al.* 1998) using the Myc-tag forward primer and Myc-tag reverse primer. His$^+$ integrants were verified by colony PCR. The *RIF2* single amino acid mutants at the endogenous *RIF2* locus were tagged with V5 epitope and constructed in the *RIF2*-V5 epitope-tagged plasmid pHK70. The plasmid was assembled according to the protocol: "Creating Insertions or Deletions Using Overlap Extension PCR Mutagenesis" (Green and Sambrook 2012). This construct was made in two steps using plasmid p406-Rif2 described above that contains the *RIF2* coding region flanked by 245 bp of genomic sequences. The primers used for each of the steps are given in parentheses. The first step amplified the C terminus of *RIF2* together with a glycine 8 (G8) linker (HK3, HK4), a unique *Not*I site (HK7, HK9), and V5 tag from pLenti6/UbC/V5-DEST Gateway Vector (Life Technologies) (HK5, HK6), which was cloned into p406-Rif2 cut with *Bsp*EI/*Not*I, creating pHK1. The second step used overlap extension to amplify the genomic region downstream of *RIF2* (HK18, HK19), adjacent to the upstream region of *RIF2* (HK20, HK15), and p406-Rif2 backbone, which included a *Kpn*I site (HK16, HK17). This step removed some of the upstream region of *RIF2* retaining a unique *Bsr*GI site. After assembly, this product was cloned into pHK1 cut with restriction enzymes *Bsr*GI and *Kpn*I, creating pHK70. The product was sequence verified. Proper chromosomal integration of epitope-tagged *RIF2* and *NAAIRS* mutants was confirmed by PCR.

### Generation of single amino acid rif2 mutants

Single amino acid changes in the N-terminal region at positions 2–49 were generated in *RIF2* in the plasmid pHK70 according to "Protocol 3: *In Vitro* Mutagenesis Using Double-Stranded DNA Templates: Selection of Mutants with *Dpn*I" (Green and Sambrook 2012). To expedite this mutagenesis, some of the point mutants (pHK28–34, pHK37–64) were made by GENEWIZ. The region of each construct containing a *rif2* mutation was PCR amplified and sequenced to confirm the presence of the desired mutation. Plasmids containing the *rif2* mutants were cut using *Afe*I (except where indicated otherwise) and targeted to the *RIF2* endogenous locus in OAy1002 by recombination. In cases where the mutation created an *Afe*I site (pHK3, pHK5–27, pHK51) plasmids were digested using *Bsr*GI and integrated at the *RIF2* locus in OAy1002. Proper integration of the *rif2* mutants at the endogenous *RIF2* locus was confirmed by PCR and verified by sequencing.

### RAP1–RIF2$_{60}$ fusion constructs integrated at the RAP1 locus

We used Gibson assembly (Gibson 2011) to generate the integrating plasmid pHK35, containing the *RAP1–RIF2*$_{60}$ fusion gene. The final construct, based in the pRS405 vector, contains the following elements stitched together: the C-terminal region of *RAP1* amplified from genomic DNA, fused to a flexible glycine 10 (G10) linker (HK89, HK98); the N-terminal 60 aa of Rif2, including a stop codon, from p406-Rif2 (HK97, HK94); the 250-bp *CYC1* terminator from p414-GALS (ATCC87344) (HK117, HK118); the *URA3* cassette from p406-Rif2 (HK93, HK96); and 176 bp of genomic DNA 3′ of *RAP1* to target to the construct to the *RAP1* locus (HK95, HK90). The construct was sequence verified and then digested

with *Sac*I/*Not*I and integrated at the *RAP1* locus in CVy245 or HKy639. Ura$^+$ integrants were verified by colony PCR, sporulated, and tetrads were analyzed. Strains with the desired genotypes were selected for Southern and Western analysis.

The shorter version of the fusion protein, Rap1–Rif2$_{36}$, was created from pHK35 using the mutagenesis method described above for the generation of single amino acid changes removing codons 37–60 (HK121, HK123) to create pHK68. The plasmid was sequence verified, digested with *Sac*I/*Not*I, and then integrated at the *RAP1* genomic locus in HKy639. Ura$^+$ integrants were verified by PCR and diploids were sporulated to generate haploid cells of the specific genotype.

The mutant *RAP1–RIF2$_{60}$ F8A*, *F8Y*, and *F8W* fusion genes were created using the site-directed mutagenesis method described above for the generation of single amino acid changes using pHK35 as a template. The resulting plasmids (pHK65, pHK74, and pHK73, respectively) were sequenced, and those containing the desired mutations were digested with *Sac*I/*Not*I and integrated at the *RAP1* genomic locus. Proper integration of the RAP1 fusion genes was verified by colony PCR and sequencing.

The *RAP1ΔC–RIF2$_{60}$* fusion gene was created using Gibson assembly of two fragments: the region amplified from genomic DNA, which removes 498 bp from the end of *RAP1* at amino acid 662 (HK128, HK129), and the region from pHK35, which contains the glycine10 linker-RIF2$_{60}$-*CYC1* components (HK130, HK131) that were reassembled into pHK35 cut with *Not*I/*Bgl*II, creating pHK72. After sequence verification, the fusion construct was digested with *Not*I/*Sac*I and introduced into the *RAP1* genomic locus in HKy639 selecting Ura$^+$ integrants (HKy768, HKy769). As a control, a construct containing only *rap1ΔC* (HK128, HK132) that truncated the *RAP1* gene at codon 662 was engineered in a similar fashion, creating pHK71. This plasmid was sequence verified and integrated at the *RAP1* genomic locus in HKy639 selecting Ura$^+$ integrants (HKy754, HKy755).

### Generation of RIF1, XRS2, and TLC1 deletion strains

To generate the *RIF1* deletion, the *LEU2* cassette was amplified from pRS405 (OCC85, OCC86) (Brachmann *et al.* 1998) and integrated into the *RIF1* locus of CVy245, yielding HKy639. Leu$^+$ integrants were verified by PCR before tetrad analysis. A diploid yeast strain containing *XRS2/xrs2ΔCt* (yYM311), previously generated in our laboratory (Ma and Greider 2009), was transformed to delete the *RIF2* locus using a PCR product containing the *LEU2* cassette from pRS405 (OCC122, OCC123) (Brachmann *et al.* 1998) to generate JHUy912. The Rap1–Rif2$_{60}$ fusion was introduced into these strains by transformation to replace the *RAP1* locus as described above.

A deletion of *TLC1* was introduced into *RIF2/rif2Δ*, *RAP1/rap1*::*(Rap1–Rif2$_{60}$–URA3)* (HKy551) by transformation of a PCR product from yeast strain YCC115 containing a *tlc1-Δ*::*LEU2* cassette (OCC168, OCC171) to generate two independent diploids HKy668 and HKy669. The Leu$^+$ integrants were verified by PCR.

### Southern analysis and telomere length measurement

Strains for telomere length analysis were grown overnight at 30° in liquid medium yeast extract-peptone-dextrose (YPD). Five $OD_{600}$ of cells were collected per sample and washed with water. Genomic DNA was prepared from each strain as follows: Cell pellets were ruptured by 8 min of vigorous shaking (Eppendorf mixer 5432) in equal volumes of 0.5 mm glass beads (Biospec Products), phenol-chloroform (50:50), and lysis buffer [1% sodium dodecyl sulfate (SDS), 2% Triton X-100, 100 mM sodium chloride (NaCl), 10 mM Tris, pH 8.0, 1 mM ethylenediamine tetracetic acid (EDTA)]. DNA was precipitated in ethanol and resuspended at 37° in TE (10 mM Tris, pH 8.0, 1 mM EDTA) and RNaseA (10 μg/ml). Samples were digested with *Xho*I and separated by electrophoresis on a 1% agarose gel in 1× TTE buffer (20× = 1.78 M Tris base, 0.57 M taurine, 0.01 M EDTA). On each gel, 250 ng of 2-log DNA ladder (NEB N3200) was included as a reference. After electrophoresis was complete, the gel was denatured for 30 min [0.2 M sodium hydroxide (NaOH), 0.34M NaCl] and neutralized (1.5 M NaCl, 0.5 M Tris, pH 7.0) for 30 min before vacuum transfer (Boekel Appligene vacuum blotter) at 50 mbar onto Amersham Hybond-N+ membrane (GE Healthcare) in 10× SSC (1.5 M NaCl, 0.17 M sodium citrate) for 1 hr. After UV-crosslinking (UV Stratalinker 2400, Stratagene), the membrane was prehybridized for 1–2 hr in Church buffer (0.5 M Tris, pH 7.2, 7% SDS, 1% bovine serum albumin, 1 mM EDTA) and hybridized with a radiolabeled subtelomeric Y′ fragment (750-bp fragment generated by PCR from yeast genomic DNA using primers YPrimeFWD and YPrimeREV) and radiolabeled 2-log DNA ladder probe. Hybridized nylon membranes were exposed to Storage Phosphor Screens (GE Healthcare) and scanned on a Storm 825 imager (GE Healthcare). The images were converted using Adobe Photoshop CS6 and adjusted for contrast using the curves feature within the software. In the represented Southern blots, the numbers on the *x*-axis indicate the sizes of the 2-log ladder in kilobases. The numbers on the *y*-axis represent the lane numbers in the agarose gel.

### Western blot analysis

Yeast strains were grown at 30° in YPD until $OD_{600}$ reached 0.4–0.6. Whole cell protein lysates were prepared by trichloroacetic acid (TCA) extraction as follows: three $OD_{600}$ of cells were collected and resuspended in 10 ml of 10% TCA for 30 min. After centrifugation, the TCA-treated cells were resuspended in 1 ml 1 M HEPES buffer, pH 7.5 and transferred into a microcentrifuge tube. Cells were pelleted and resuspended in 50 μl 2× SDS-polyacrylamide gel electrophoresis (PAGE) sample buffer [125 mM Tris, pH 6.8, 4% SDS, 20% glycerol, 0.2 M dithiothreitol (DTT), 0.012% bromophenol blue dye (BPB)] then ruptured with an equal amount of 0.5 mm glass beads for 3 min on a high-speed vortex mixer. An additional 50 μl of 2× SDS-PAGE buffer was added to each sample, followed by 5 min at 100° and 15 sec of vigorous shaking. The samples were centrifuged for

10 min at top speed in a microcentrifuge and the supernatant was collected and stored at −20°.

Whole cell lysate (3 μl) was loaded per lane on a 10% TGX SDS-PAGE gel (Bio-Rad) along with molecular weight protein standards (Bio-Rad no. 161-0373) and resolved by electrophoresis. The proteins were transferred to 0.45 μm Immobilon-FL membrane (Millipore) according to recommended protocol (Bio-Rad). All Blue, Precision Plus protein standards (Bio-Rad no. 161-0373) were used as molecular weight markers. All transferred membranes were blocked in Odyssey blocking buffer (LI-COR) for 1 hr at room temperature (RT). The membranes were washed three times in 1× wash buffer (10 mM Tris, pH 8.0, 150 mM NaCl, 0.1% Triton X-100, 0.01% IGEPAL CA-630; Sigma) for 15 min, 5 min, and 5 min at RT. When using LI-COR detection, the final wash contained no detergents (1× TBS: 10 mM Tris, pH 8.0, 150 mM NaCl). The 13xMyc epitope was detected with a 1:10,000 dilution of anti-Myc 9E10 antibody (National Cell Culture Center, Minneapolis). Anti-actin (1:500 dilution of Anti-actin; Sigma A2066) and anti-PGK (1:10,000 dilution of anti-PGK; Invitrogen 459250) antibodies served as loading controls. The appropriate species IRDye secondary antibodies (LI-COR) were diluted at 1:15,000 in Odyssey blocking buffer and incubated for 2 hr at RT. Immunoblots were analyzed on an Odyssey infrared imaging system (LI-COR Biosystems) using the quantification software provided. The Rif2 protein levels of the samples were compared to the actin or the PGK loading control; this ratio in the wild type (WT) was set to 1 and the other samples were normalized to this value. The Rif2 protein level from two independent haploids was determined, and the average of these two values is reported in Figure 1.

The V5 epitope was detected with a 1:2000 dilution of anti-V5 antibody (Invitrogen no. 460705) for 1 hr at RT. Anti-mouse immunoglobin G horseradish peroxidase (IgG-HRP)-linked secondary antibody (Cell Signaling Technologies no. 7076) was diluted 1:10,000 in 5% milk (Bio-Rad), 0.05% Triton X-100, and incubated for 45 min at RT. SuperSignal West Femto Maximum Sensitivity Substrate (Thermo Scientific no. 34095) was used to detect the chemiluminescent signal on an ImageQuant LAS4000 mini (GE Healthcare). Since the loading control comigrated with the V5-tagged Rif2, the blots were stripped with Restore Western Blot Stripping Buffer for 25 min at room temperature (Thermo Scientific no. 21059), washed three times in 1× TBS as described above, and verified that no signal was present. After treating 30 min to 1 hr in Odyssey blocking buffer, the membranes were then incubated for 1 hr at RT with 1:10,000 of anti-PGK using the same IgG-HRP-secondary antibody as described. The Rif2 protein levels of the samples and loading controls were quantitated using ImageJ (Schneider *et al.* 2012) and normalized relative to WT levels.

### *Data availability*

All strains and plasmids described here and in the Supporting Information are available upon request.

## Results

### *Scanning mutagenesis of RIF2*

To better understand the role of Rif2 in telomere length maintenance, we scanned the entire coding region of *RIF2*, substituting every 6 contiguous codons with a sequence encoding NAAIRS (Lonergan *et al.* 1998), generating a set of 66 *rif2–NAAIRS* mutants. The mutations were named for the first codon where the substitution begins. For example, NAAIRS2 substitutes codons 2–7, and NAAIRS8 substitutes codons 8–13. Each mutant was integrated into the yeast genome at the *URA3* locus in a *RIF2/rif2Δ* heterozygous diploid and verified by sequencing. Wild-type *RIF2* integrated at *URA3*, as a control, was able to complement a *rif2Δ* (data not shown). Telomere length was examined in *rif2Δ*::*kanMX4 ura3-1*::*rif2NAAIRS-URA3* haploid segregants by Southern blot and classified as wild type, long (similar to *rif2Δ*), or medium (between *rif2Δ* and wild type). There were a number of regions in *RIF2* where *NAAIRS* mutations resulted in a long telomere phenotype similar to *rif2Δ* (Figure 1 and Figure S1).

To determine whether the mutant proteins were expressed at wild-type levels, we tagged each of the mutants that showed long telomeres with a 13xMyc tag and quantified Rif2 protein levels by Western analysis. As a control, we tagged a wild-type copy of *RIF2* integrated at the *URA3* locus and showed the 13xMyc tag did not affect telomere length (Figure S2A). A number of the NAAIRS substitutions resulted in significantly reduced protein expression; for example, the mutations NAAIRS212 and NAAIRS338 (Figure S1A), disrupted protein stability, suggesting the long telomeres in these mutants were likely due to low Rif2 levels. However, there was a distinct subset of mutants in which wild-type or near wild-type protein levels were present and yet the NAAIRS substitution resulted in longer than wild-type length telomeres (Figure 1). Strikingly, 7 of 11 of the long or medium length mutants that expressed at least 50% protein levels were in the N-terminal domain of Rif2. We thus focused our attention on this N-terminal region.

While this work was underway, the Thoma lab reported the crystal structure of Rif2 protein and Rif2 complexed with the C-terminal domain of Rap1 (Shi *et al.* 2013). Rif2 contains a large central AAA+ domain with Walker A and Walker B motifs. The crystal structure revealed a C-terminal domain in Rif2 that interacts with Rap1 (Figure 2A). The N-terminal domain of the Rif2 protein from amino acid (aa) 1–60 was mostly unstructured but contained a short helix from T37-K48 called the **R**ap1 **B**inding **M**otif (RBM). A peptide spanning Rif2 residues 30–49 bound to the Rap1 C-terminal domain in solution. This peptide has two residues, L42 and L44, which have crystal contacts with the Rap1 C-terminal domain, while residues 49–60 were unstructured (Shi *et al.* 2013). As mentioned above, the block of NAAIRS mutations that affected protein function (NAAIRS2–NAAIRS44) was located in this unstructured N-terminal domain of Rif2.

| Mutant | Phenotype | Protein expression |
|---|---|---|
| NAAIRS2 | long | medium (0.52) |
| NAAIRS8 | long | WT (1.49±0.12) |
| NAAIRS14 | long | WT (0.74±0.03) |
| NAAIRS20 | long | medium (0.53±0.01) |
| NAAIRS26 | medium | WT (0.78±0.14) |
| NAAIRS32 | long | low (0.44±0.03) |
| NAAIRS38 | medium | WT (2.12±0.52) |
| NAAIRS44 | medium | WT (0.95±0.13) |
| NAAIRS50 | wt | |
| NAAIRS56 | wt | |
| NAAIRS62 | wt | |
| NAAIRS68 | wt | |
| NAAIRS74 | long | low (0.34±0.11) |
| NAAIRS80 | medium | medium (0.55±0.44) |
| NAAIRS86 | long | medium (0.52±0.03) |
| NAAIRS92 | wt | |
| NAAIRS98 | long | low (0.29±0.04) |
| NAAIRS104 | long | low (0.29±0.04) |
| NAAIRS110 | long | low (0.15±0.06) |
| NAAIRS116 | long | low (0.00±0) |
| NAAIRS122 | medium | WT (1.00±0.01) |
| NAAIRS128 | medium | low (0.19±0.04) |
| NAAIRS134 | wt | |
| NAAIRS140 | medium | low (0.33±0.04) |
| NAAIRS146 | wt | |
| NAAIRS152 | wt | |
| NAAIRS158 | wt | |
| NAAIRS164 | wt | |
| NAAIRS170 | wt | |
| NAAIRS176 | wt | |
| NAAIRS182 | wt | |
| NAAIRS188 | wt | |

| Mutant | Phenotype | Protein expression |
|---|---|---|
| NAAIRS194 | medium | low (0.33±0.03) |
| NAAIRS200 | wt | |
| NAAIRS206 | long | low (0.00±0) |
| NAAIRS212 | long | low (0.37±0) |
| NAAIRS218 | wt | |
| NAAIRS224 | wt | |
| NAAIRS230 | long | low (0.16±0.02) |
| NAAIRS236 | long | low (0.19±0.04) |
| NAAIRS242 | long | low (0.23±0.09) |
| NAAIRS248 | long | low (0.11±0.02) |
| NAAIRS254 | wt | |
| NAAIRS260 | wt | |
| NAAIRS266 | wt | |
| NAAIRS272 | long | low (0.00±0) |
| NAAIRS278 | wt | |
| NAAIRS284 | wt | |
| NAAIRS290 | long | low (0.00±0) |
| NAAIRS296 | long | low (0.22±0.04) |
| NAAIRS302 | wt | WT (0.81±0.12) |
| NAAIRS308 | long | low (0.00±0) |
| NAAIRS314 | wt | |
| NAAIRS320 | long | low (0.38±0) |
| NAAIRS326 | medium | low (0.32±0.01) |
| NAAIRS332 | medium | low (0.22±0.06) |
| NAAIRS338 | medium | low (0.26±0.04) |
| NAAIRS344 | long | low (0.38±0.06) |
| NAAIRS350 | medium | low (0.18±0.03) |
| NAAIRS356 | long | low (0.02±0.01) |
| NAAIRS362 | long | low (0.20±0.02) |
| NAAIRS368 | medium | low (0.50±0.03) |
| NAAIRS374 | long | low (0.00±0) |
| NAAIRS380 | wt | |
| NAAIRS386 | medium | WT (0.83±0.04) |
| NAAIRS392 | wt | |

**Figure 1** Summary of telomere length and protein expression in *rif2–NAAIRS* mutants. The telomere length of each of the *rif2–NAAIRS* mutants was categorized as wild-type (WT), medium, or long. For mutants with medium or long telomeres, the *rif2–NAAIRS* construct was tagged with the 13xMyc epitope and the relative level of Rif2 protein was measured by Western analysis. For each mutant, protein level in two independent haploids was measured and normalized to the loading control and to wild-type Rif2 protein levels (see *Materials and Methods*). Each mutant was characterized as having WT (>70%), medium (50–70%), or low expression level (0–50%). Highlighted mutants indicate those with either WT or medium Rif2 expression level and telomeres longer than WT. *NAAIRS* mutants that had WT telomere length were not retested to examine protein levels. Representative examples of Southerns and Westerns for these mutants are shown in Figure S1.

### *N-terminal rif2 point mutants have long telomeres*

The N-terminal region of Rif2 is highly conserved among *Saccharomyces* (Figure 2B). To probe this region more closely, we substituted each individual residue from aa 2–37 with alanine (or a different residue if alanine was the wild-type residue). These point mutants were tagged with a V5 epitope and integrated at the *RIF2* genomic locus in haploid cells. The telomere length of two independent transformants of each mutant was compared to four controls: wild type, *RIF2*, *rif2Δ*, and the original NAAIRS mutant haploid strain (Figure 2C and Figure S3). Control experiments showed that the V5 tag did not affect telomere length at the wild-type *RIF2* locus (Figure S2B). If discordant results were obtained with two independent transformants, additional transformants were analyzed to determine the effect of that mutant.

Mutations in six residues in the N-terminal region resulted in telomere elongation: D5, F8, I11, R12, R13, and D29 (Figure 2C and Figure S2C, also see Figure S3). Mutants in F8, I11, R12, and R13 were expressed at or just above wild-type levels, while D5 and D29 were slightly reduced (Figure S2D). All of these residues fall within the unstructured region in the crystal structure (Shi *et al.* 2013). Remarkably, the single amino acid change F8A showed significant telomere lengthening comparable to both the six-codon change in *rif2–NAAIRS8* and *rif2Δ* (Figure 2C), suggesting this is a key residue in Rif2 that is critical for telomere length regulation. In addition to residues with a major effect, there were also residues that had smaller effects. For some NAAIRS mutants, such as *rif2–NAAIRS14* and *rif2–NAAIRS20*, none of the single mutants affected telomere length, however when all six codons were mutated in combination, telomere lengthening was observed (Figure S3). These results are consistent with this region being a binding site for some protein, in which docking of the F8 residue is the most critical, and neighboring residues contribute to the interaction.

### *The N-terminal domain of Rif2 mediates telomere length regulation*

Because the mutants in the N terminus of Rif2 mimic loss of function of the Rif2 protein, we next asked whether this

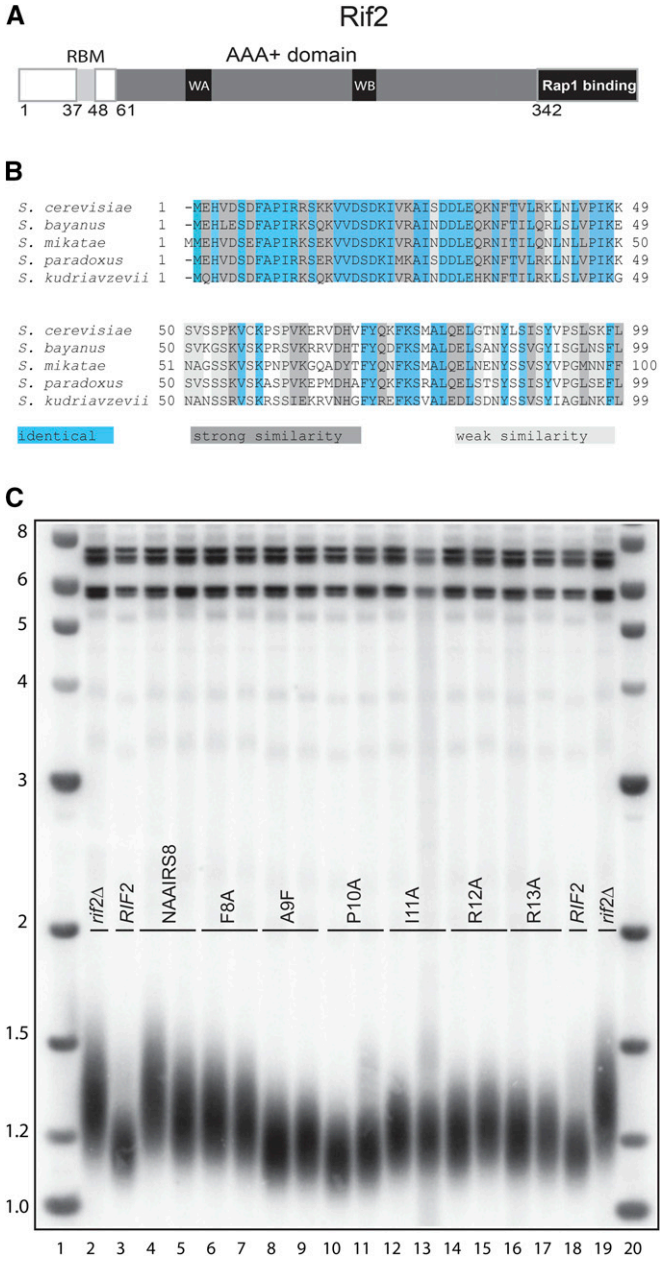


**Figure 2** Point mutants in *RIF2* disrupt protein function. (A) The domain structure of Rif2 protein is shown. The C-terminal region binds Rap1. There is an AAA+ domain that contains Walker A and B motifs (designated WA and WB). The N-terminal domain is not well structured but contains a short helix (RBM) that interacts with Rap1. The regions in white have no known structure. (B) The alignment of residues in the Rif2 N-terminal region from five *Saccharomyces* species is shown. Identical residues are highlighted in blue, those residues with strong similarity are in dark gray, and those with weak similarity in light gray. (C) Southern blot analysis of telomeres from *rif2–NAAIRS8* and the six individual mutations within the *rif2–NAAIRS8* mutant. The size markers on the side represent kilobases. Two independent haploid transformants for each single point mutant are shown.

N-terminal domain would function alone if tethered at the telomere. We generated a fusion gene encoding the N-terminal 60 codons of *RIF2* fused to the C terminus of *RAP1*. We will refer to this construct as *RAP1–RIF2*$_{60}$ and to the resulting fusion protein as Rap1–Rif2$_{60}$ (Figure 3A). We chose the N-terminal 60 aa of Rif2 because in the crystal structure the well-structured protein begins at residue 61. To promote flexibility of the fusion domain, we added a glycine linker sequence between Rap1 and the Rif2$_{60}$ N-terminal domain. The *RAP1–RIF2*$_{60}$ construct was transformed into a *RIF2/rif2Δ* heterozygous diploid and integrated at the *RAP1* genomic locus. *RIF2/rif2Δ*, *RAP1/RAP1–RIF2*$_{60}$ double heterozygotes were sporulated and telomere lengths were examined in two independent spores as well as in the diploids. Remarkably, the *RAP1–RIF2*$_{60}$ construct fully suppressed the telomere lengthening in a *rif2Δ* mutant (Figure 3B, lanes 4 and 5). Moreover, this domain dominantly shortened telomeres since telomeres were shorter in the heterozygous diploid *RIF2/rif2Δ* containing the *RAP1–RIF2*$_{60}$ construct than in the parental diploid (Figure 3B, lanes 2 and 3). This shortening effect was also observed in haploid cells. Wild-type cells expressing the fusion had telomeres shorter than wild-type cells without the fusion (Figure 3B, lanes 6 and 7). This gain-of-function effect may result from alteration of the regulated cell cycle dissociation of Rif2 from the telomere (Smith *et al.* 2003), as discussed below. The suppression of the *rif2Δ* phenotype by the *RAP1–RIF2*$_{60}$ construct suggests that tethering this functional domain of Rif2 at the telomere blocks excessive telomere elongation.

Rif1 and Rif2 act through different pathways to limit telomere extension (Wotton and Shore 1997). To test whether the *RAP1–RIF2*$_{60}$ construct would also block *rif1Δ* telomere elongation, we generated a triple heterozygous diploid: *RIF1/rif1Δ*, *RIF2/rif2Δ*, *RAP1/RAP1–RIF2*$_{60}$. Telomere length was measured in two independent haploids of each genotype (Figure 3C). The Rap1–Rif2$_{60}$ fusion protein fully suppressed the long telomeres in both *rif1Δ* and *rif1Δ rif2Δ* mutants.

We noted that there was a slight difference in telomere length in *rif1Δ rif2Δ* cells compared to *rif2Δ* cells expressing the fusion construct (Figure 3C, compare lanes 10 and 11 to lanes 18 and 19). To test whether this difference was due to insufficient cell divisions needed to reach steady state, we passaged cells four times in subcultures. The telomere length of each mutant expressing the fusion protein was stable over the successive passages (Figure S4). The slight difference in final telomere length in *rif1Δ* or *rif2Δ* mutants expressing the *RAP1–RIF2*$_{60}$ construct might reflect the fact that Rif1 affects telomere length through a different pathway than Rif2 (Wotton and Shore 1997).

To determine whether telomere shortening in cells expressing the *RAP1–RIF2*$_{60}$ construct was working through the telomerase pathway we deleted the telomerase RNA component, *TLC1*, in a *RIF2/rif2Δ*, *RAP1/RAP1-RIF2*$_{60}$ diploid. Telomere elongation in *rif2Δ* mutants was blocked by the loss of telomerase (Figure S5), as shown previously (Teng *et al.* 2000). Expression of the *RAP1–RIF2*$_{60}$ fusion in *tlc1Δ* had little effect on telomere length, while *tlc1Δ rif2Δ* cells not expressing the fusion construct had slightly longer telomeres than those expressing the construct (Figure S5A, compare lanes 10 and 11 to lanes 12 and 13). While this slight

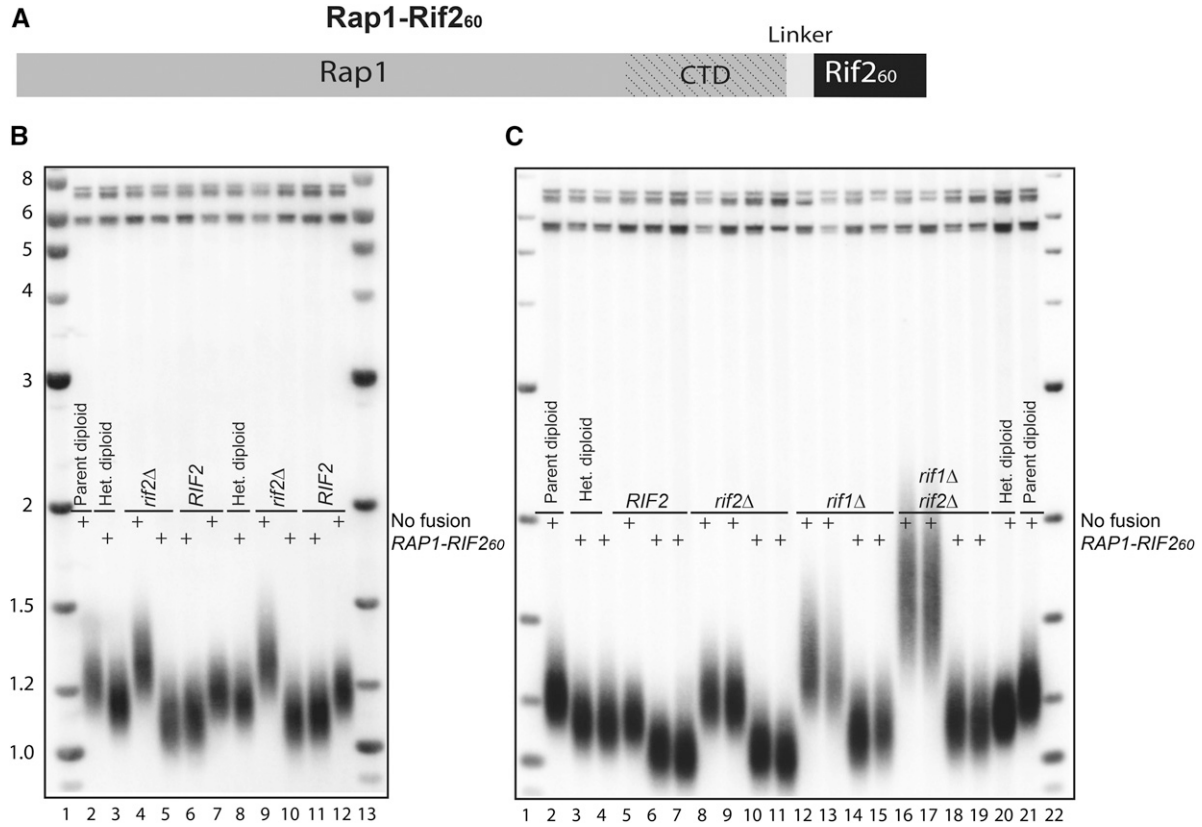


**Figure 3** Rap1–Rif2$_{60}$ fusion protein blocks telomere elongation. (A) Schematic of Rap1–Rif2$_{60}$ fusion protein. The full-length *RAP1* coding region was fused in frame to a glycine 10 linker followed by the first 60 codons of *RIF2*. (B) *rif2Δ* mutants expressing the *RAP1–RIF2$_{60}$* construct. The genotype of the strain is indicated in each lane and the presence or absence of the fusion protein is shown with a + sign in each lane. The parental diploid was transformed with the fusion construct to yield the heterozygous diploid (Het. diploid) and was dissected to generate the haploid segregants. (C) Expression of *RAP1–RIF2$_{60}$* construct in *rif1Δ* mutants and *rif1Δ rif2Δ* mutants. The genotype of the strain is indicated in each lane and the presence or absence of the fusion protein is show with a + sign. The size markers on the side represent kilobases.

difference could be due to effects of the fusion protein on other telomere maintenance pathways, we suspect it is due to increased telomere recombination in the *tlc1Δ rif2Δ* cells. The loss of Rif2 in a telomerase mutant has previously been shown to promote recombination and accelerate survivor formation (Teng *et al.* 2000; Chang *et al.* 2011; Ballew and Lundblad 2013; Hu *et al.* 2013). We found that the rapid appearance of survivors in *tlc1Δ rif2Δ* cells led to slightly longer bulk telomere bands than *tlc1Δ* (Figure S5B, compare lanes 4 and 5 to lanes 6 and 7). Expression of the fusion construct may delay telomere recombination. Taken together, the telomere shortening caused by the Rap1–Rif2$_{60}$ fusion protein and the requirement for telomerase indicate that this small domain of Rif2 can block telomere overelongation by telomerase in both *rif1Δ* and *rif2Δ* mutants. We will refer to this functional N-terminal domain as the BAT domain for **B**locks **A**ddition of **T**elomeres.

### *The function BAT domain does not require interaction with the RAP1 C-terminal domain*

The N-terminal 60 amino acids of Rif2 include a small helical domain termed RBM between positions T37 and K48 that makes crystal contacts with the C-terminal domain of Rap1 (Shi *et al.* 2013). To determine whether the binding to the Rap1 C terminus is required for the function of the BAT domain we took two approaches: first, we removed the C terminus of Rap1, and second, we created a fusion protein with a shorter version of the BAT domain that lacks the RBM region (Figure 4A).

We generated a new fusion construct (termed rap1*ΔC–RIF2$_{60}$*) in which the Rap1 C terminus is truncated at amino acid 662 with the Rif2 BAT domain fused to the Rap1 DNA binding domain. The expression of the rap1*ΔC–RIF2$_{60}$* fusion completely suppressed the long telomere phenotype in *rif1Δ*, *rif2Δ*, and *rif1Δ rif2Δ* mutants (Figure 4B). This result indicates the BAT domain does not need the Rap1 C terminus to block telomere elongation. As a control, in the same strain, we generated a Rap1ΔC-truncated at amino acid 662 that lacks Rif2 BAT domain. As expected, expression of the Rap1-ΔC-truncation showed long telomeres and did not rescue telomere length in *rif1Δ*, *rif2Δ*, or *rif1Δ rif2Δ* (Figure S6).

Next we examined a fusion with a shortened BAT domain, rap1*ΔC–RIF2$_{36}$*, which lacks the RBM residues (Figure 2). Expression of Rap1–Rif2$_{36}$ fully blocked telomere elongation in *rif1Δ*, *rif2Δ*, and *rif1Δ rif2Δ* mutants (Figure 4, C and D). While this *RAP1–RIF2$_{36}$* construct restored wild-type telomere

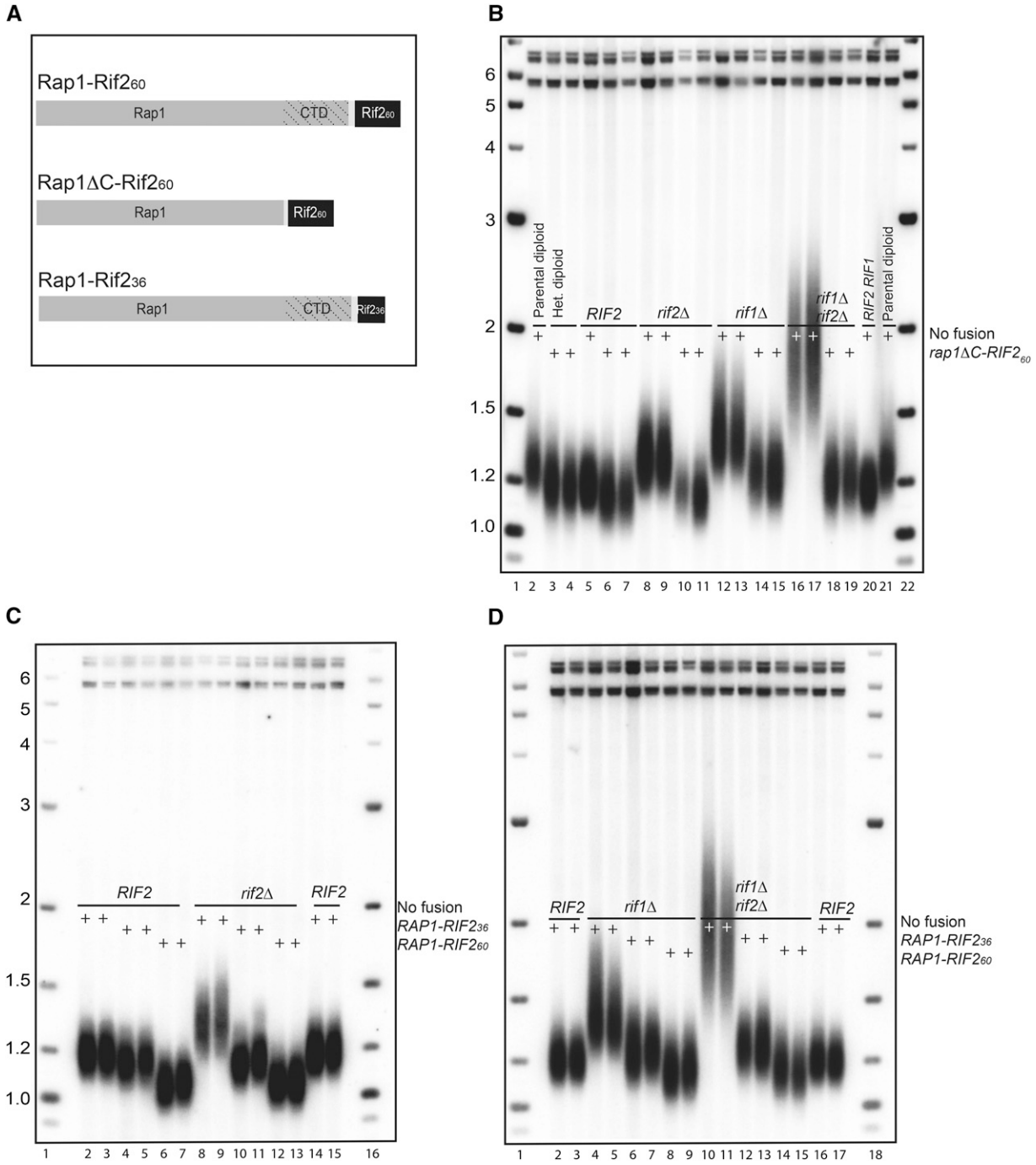


**Figure 4** The C-terminal domain of Rap1 is not required for BAT domain function. (A) Schematic of three fusion protein constructs. (B) *rif1Δ*, *rif2Δ*, and *rif1Δ rif2Δ* double mutants expressing *rap1ΔC–RIF2*$_{60}$ construct were analyzed by Southern blot. The genotype of the strain is indicated above each lane and the presence or absence of the fusion construct is shown with a + sign in each lane. (C) *rif2Δ* mutants expressing the fusion construct with a shortened Rif2 N terminus, *RAP1–RIF2*$_{36}$. The genotype of the strain is indicated above each lane and the presence or absence of either the *RAP1–RIF2*$_{36}$ construct or *RAP1–RIF2*$_{60}$ construct is shown with a + sign. (D) *rif1Δ* and *rif1Δ rif2Δ* double mutants expressing the shortened Rif2 N terminus, *RAP1–RIF2*$_{36}$. The genotype of the strain is indicated above each lane and the presence or absence of either the *RAP1–RIF2*$_{36}$ construct or the *RAP1–RIF2*$_{60}$ construct is shown with a + sign. The size markers on the side represent kilobases.

length, it did not cause shortening below wild-type length like the *RAP1–RIF2*$_{60}$ construct (Figure 4, C and D). This lesser degree of telomere shortening by the *RAP1–RIF2*$_{36}$ compared to the *RAP1–RIF2*$_{60}$ could be due to a slightly reduced accessibility or flexibility of this shorter domain. The lack of requirement for the Rap1 C-terminal domain, together with the ability of the *RAP1–RIF2*$_{36}$ to fully restore wild-type telomere length, suggest that the BAT domain of Rif2 does not require the presence of the Rap1 C terminus to affect telomere shortening.

### *XRS2 C terminus does not mediate the function of the Rif2 BAT domain*

Recent studies have suggested that Rif2 binds to the C-terminal region of Xrs2 and that this blocks Tel1 telomere association, thereby limiting telomere elongation (Hirano *et al.* 2009). To determine whether the C-terminal domain of *XRS2* is required for the ability of the BAT domain to limit telomere length, we introduced the *RAP1–RIF2*$_{60}$ construct into a doubly heterozygous strain *RIF2Δ/rif2Δ XRS2/xrs2ΔCt* expressing an Xrs2 C-terminal truncation protein that fails to bind Tel1 (Ma and Greider 2009) and examined telomeres in the single and double mutant haploid segregants. Expression of the Rap1–Rif2$_{60}$ fusion protein resulted in significant shortening in the *rif2Δ xrs2ΔCt* cells (Figure 5, lanes 16 and 17). These results suggest that the Rif2 BAT domain can regulate telomere length independent of the Xrs2 C-terminal domain.

### *Mutations at F8 abolish the shortening effect of the Rap1–Rif2$_{60}$ fusion protein*

In the NAAIRS scanning mutagenesis experiments, we identified the F8 residue as playing a major role in Rif2 function. To determine if this amino acid was also important in the effect of the Rap1–Rif2$_{60}$ protein, we made a fusion construct containing this F8A substitution. When this mutant *RAP1–rif2$_{60}$ [F8A]* fusion construct was expressed in a *rif2Δ* background, telomere shortening did not occur (Figure 6A, lanes 14 and 15), indicating the *RAP1–rif2$_{60}$ [F8A]* mutation renders the BAT domain nonfunctional. Curiously, long telomeres were seen when the *RAP1–rif2$_{60}$ [F8A]* fusion construct was expressed in wild-type haploids (Figure 6A, lanes 9 and 10), suggesting that tethering the mutant BAT domain to Rap1 dominantly interferes with normal length regulation. Since this construct is the only copy of *RAP1* in the cell, all of the telomeres should be bound by the Rap1–Rif2$_{60}$ [F8A] protein and thus may interfere with the function of the wild-type Rif2.

### *Aromatic amino acid tryptophan can mimic phenylalanine at F8*

The functional importance of the *F8A* mutation in both the *RIF2* gene and in the *RAP1–rif2$_{60}$ [F8A]* fusion suggests this region may be a protein–protein interaction site. To test whether aromatic phenylalanine may be specifically recognized, we substituted this amino acid with either of the aromatic amino acids, tryptophan or tyrosine. Remarkably, the *RAP1–rif2$_{60}$ [F8W]* restored telomere shortening in *rif2Δ*, *rif1Δ*, and *rif1Δ rif2Δ* (Figure 6, C and D), indicating an aromatic amino acid can at least partially restore the function of the BAT domain. The *RAP1–rif2$_{60}$ [F8Y]* mutation more closely resembled the *RAP1–rif2$_{60}$ [F8A]* mutant, suggesting this residue may interfere with function. These experiments support the model that the F8 aromatic residue in the BAT domain is an important binding determinant for an as yet unknown protein that limits telomere elongation.

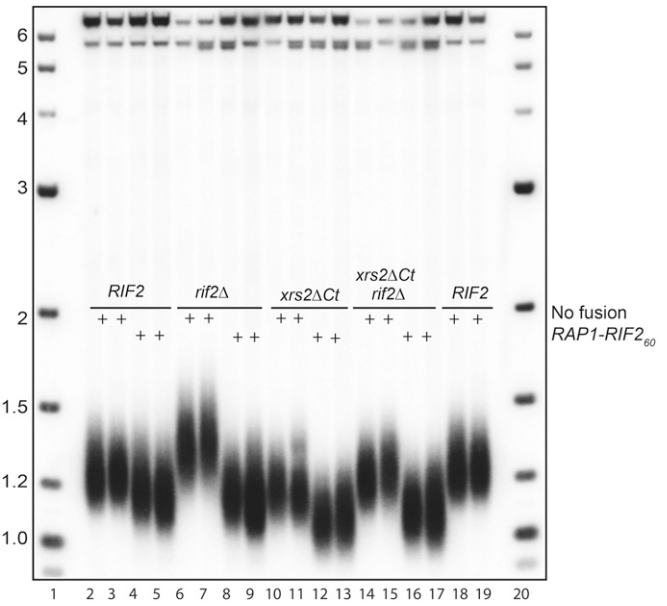


**Figure 5** Xrs2 C terminus is not required for the Rif2 BAT domain to shorten telomeres. Southern blot telomere analysis of *xrs2Δ*Ct and *rif2Δ xrs2Δ*Ct cells expressing *RAP1–RIF2$_{60}$* construct. The genotype of the strain is indicated above each lane and the presence or absence of the *RAP1–RIF2$_{60}$* construct is shown with a + sign. The size markers on the side represent kilobases.

## Discussion

To probe the mechanism of telomere length regulation, we carried out scanning mutagenesis of *RIF2* and identified an N-terminal domain that is essential for blocking telomere elongation. The substitution of a single amino acid, F8A, within the BAT domain mimicked the long telomeres in a *rif2Δ* mutant. Further, tethering this 60 amino acid domain to Rap1 fully blocked telomere elongation. The F8 residue was essential for blocking excess elongation, as the *RAP1–RIF2$_{60}$ [F8A]* fusion did not block telomere elongation in *rif2Δ* mutants. These results imply the BAT domain regulates telomere length by a similar mechanism in the context of either full-length *RIF2* or as an isolated domain tethered to *RAP1*.

### *The Rap1/Rif1/Rif2 scaffold is not essential to block telomere elongation*

Our results suggest the recently proposed molecular Velcro model for telomere length regulation may be incomplete. In this Velcro model, Rif1, Rif2, and Rap1 are suggested to generate an interlocking molecular scaffold that limits telomerase access to the telomere (Shi *et al.* 2013). Specifically Rif2 is proposed to contribute to the scaffold by bridging two Rap1 molecules, binding one through the RBM and the other through the AAA+ domain. Rif1 is likewise proposed to make contact with two Rap1 molecules to further support the scaffold. While our data do not address whether this scaffold forms in wild-type cells, they do suggest that such a structure is not required to block the elongation of telomeres by telomerase.

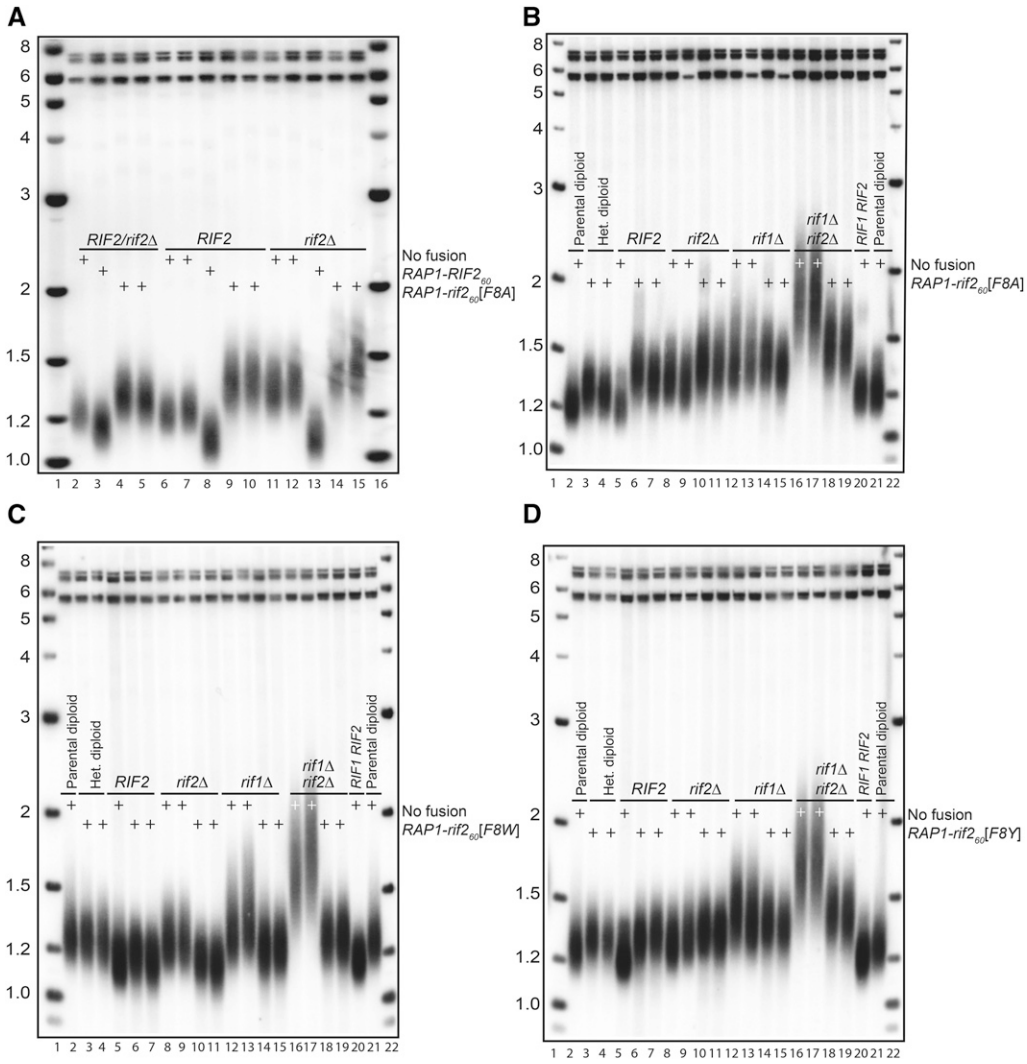


**Figure 6** Aromatic residue at position 8 is important for Rif2 BAT domain function. (A) Southern blot telomere analysis of WT and *rif2Δ* cells expressing either *RAP1–RIF2$_{60}$* or *RAP1–rif2$_{60}$ [F8A]* mutant fusion construct. The genotype of the strain is indicated above each lane and the presence or absence of the given fusion protein is shown with a + sign. (B) Southern blot telomere analysis of *RIF1 RIF2*, *rif2Δ*, *rif1Δ*, and *rif1Δ rif2Δ* mutants expressing *RAP1–rif2$_{60}$ [F8A]* fusion or no fusion. The genotype of the strain is indicated above each lane and the presence or absence of the *RAP1–rif2$_{60}$ [F8A]* is shown with a + sign. The parental diploid was transformed with the fusion construct to yield the heterozygous diploid (Het. diploid) and dissected for the haploid segregants. (C) Southern blot telomere analysis of WT, *rif2Δ*, *rif1Δ*, and *rif1Δ rif2Δ* mutants expressing *RAP1–rif2$_{60}$ [F8W]* fusion. The genotype of the strain is indicated above each lane and the presence of the *RAP1–rif2$_{60}$ [F8W]* is shown with a + sign. (D) Southern blot telomere analysis of WT, *rif2Δ*, *rif1Δ*, and *rif1Δ rif2Δ* mutants expressing *RAP1–rif2$_{60}$ [F8Y]* fusion. The genotype of the strain is indicated above each lane and the presence of *RAP1–rif2$_{60}$ [F8Y]* fusion protein is shown with a + sign. The size markers on the side represent kilobases.

### *BAT domain as a functional protein-binding site*

The modular nature of the BAT domain, and the critical F8 residue, suggests that this region of Rif2 may be a protein–protein interaction domain. The high conservation of the BAT domain in *Saccharomyces* (Figure 2B) further supports a role in protein binding. We propose that the F8 residue is the critical determinant in a binding site and that surrounding amino acids also contribute to important protein contacts. When residues near F8 were singly mutated, there was less effect on telomere length than when they were mutated together as groups of six residues (Figure 2). This additive effect was also seen in the NAAIRS2, NAAIRS14, and NAAIRS20 mutants, in which the single amino acid changes did not have as strong an effect as the group of 6 mutations (Figure S3). This finding suggests that there is a protein interaction interface over a region surrounding F8, and this aromatic residue is the key player in a protein interaction. The BAT domain may recruit an unknown protein as described below or it may interact directly with known proteins such as Cdc13, Stn1, Ten1, or telomerase to block elongation. We ruled out the Xrs2 C-terminal domain as playing a major role (Hirano *et al.* 2009) since Xrs2 C-terminal truncations still showed telomere shortening with the Rap1–Rif2$_{60}$ fusion protein.

### *The Rap1–Rif2$_{60}$ fusion causes telomere shortening*

The dominant effect of the Rap1–Rif2$_{60}$ fusion in diploid cells and its ability to shorten telomeres in haploids may be due to altered cell cycle regulation, altered affinity, loss of end protection, or a combination of these factors. The cell cycle-regulated associations of Rap1 and Rif2 with the telomere differ; Rap1 telomere association increases while Rif2 decreases in late S-phase (Smith *et al.* 2003). It may be this dissociation of Rif2 in late S-phase that allows telomere elongation. In our experiment, by tethering the functional BAT domain of Rif2 to Rap1, this dissociation at late S-phase cannot occur and thus telomere elongation may be more efficiently blocked.

The Rap1–Rif2$_{60}$ fusion also shortened telomeres in a *rif1Δ* mutant. Rif1 regulates telomere elongation through a mechanism independent of Rif2, thus the ability of the Rap1–Rif2$_{60}$ to block telomerase elongation after the loss of Rif1 suggests that the mechanism by which BAT blocks telomere elongation is not pathway specific. Experiments by Levy and Blackburn (2004) also showed that both the *rif1Δ* and *rif2Δ* long telomere phenotypes could be counteracted by overexpression of a Rap1–PDZ fusion protein that allows multimerization of Rap1. This further suggests that while Rif1 and Rif2 may normally act through different pathways, strengthening just one of those pathways may be sufficient to block telomere over elongation.

### *Putting the pieces together: a model for Rif2 BAT domain function*

Our data suggest that the BAT domain of Rif2 is a protein-binding domain that limits telomere elongation by telomerase. This domain may directly block telomere elongation or may recruit another protein that binds to the F8 residue in the BAT domain and blocks telomere elongation as depicted in Figure 7A. When Rif2 is missing, telomerase can overextend the telomeres (Figure 7B). However tethering the BAT domain directly to Rap1 restores and even strengthens the block to telomerase (Figure 7C). The specific mechanism by which the BAT domain blocks telomerase elongation is not clear; it might directly interfere with the catalytic subunit Est2 recruitment or it could affect elongation indirectly by altering telomere processing or C-strand synthesis. In addition to blocking telomerase, Rif2 plays a role in end protection. Rif2 blocks telomere recombination (Teng *et al.* 2000), thereby delaying survivors (Chang *et al.* 2011; Ballew and Lundblad 2013; Hu *et al.* 2013). Rif2 also protects telomeres from fusion (DuBois *et al.* 2002) and from nuclease processing (Bonetti *et al.* 2010a). The increased rate of telomere sequence turnover in *rif2Δ* mutants (Krauskopf and Blackburn 1996) likely reflects the combined effects of increased telomere degradation, elongation, and recombination. It is not yet clear whether the functions of Rif2 in end protection and in blocking telomerase elongation are separable or are the result of one mechanism. Our data support the role of Rif2 in blocking telomere recombination in telomerase mutants (Figure S5) and suggest that the BAT domain plays a role in this function.

### *Telomere length regulation throughout evolution*

The negative regulation of telomere elongation in length homeostasis is conserved throughout evolution. While Rif2 protein sequence is not conserved from yeast to humans, the loss of telomere binding proteins leads to telomere elongation in mammals as well (Palm and de Lange 2008). Rif2 in *S. cerevisiae* is a paralog of the conserved Orc4 protein (Byrne and Wolfe 2005). Analysis of synteny indicates that Rif2 was generated by divergence after a whole genome duplication that occurred early in the *Saccharomyces* lineage (Barnett 2004). Interestingly, the sequence conservation of *RIF2* and

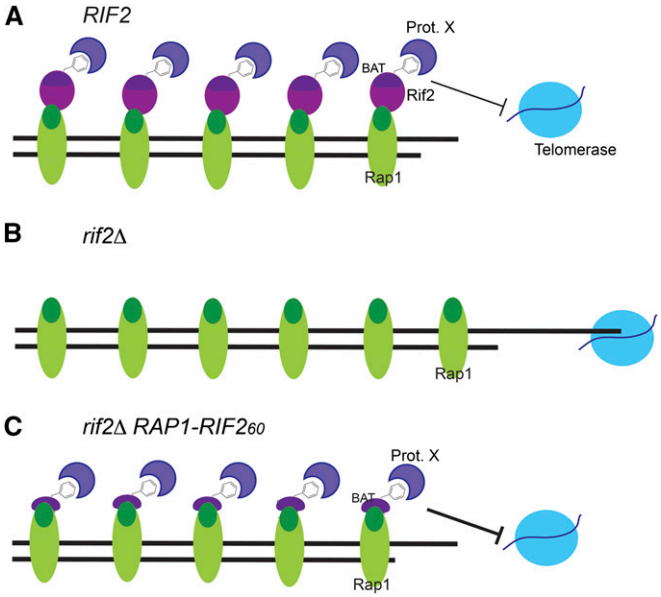


**Figure 7** Model for separation of function of Rif2 and the BAT domain. In *RIF2* cells, the Rap1 protein, shown in green, binds to the telomeric double-stranded DNA and the C-terminal domain (dark green) recruits Rif1 (not shown for simplicity) and Rif2 (purple). Rif2 binds the Rap1 C-terminal domain and blocks nuclease activity and telomerase elongation. The N-terminal BAT domain of Rif2 (dark purple) contains a critical phenylalanine residue. The F8 residue in the BAT domain serves as a protein recognition motif for a critical protein (Prot. X) that limits telomerase elongation of the telomere. (B) In *rif2Δ* telomerase elongation is not blocked by Rif2. (C) When the BAT domain is fused directly to the Rap1 C-terminal region in the *RAP1–RIF2$_{60}$* fusion construct, even in a *rif2Δ* mutant, there is strong blocking of telomerase.

*ORC4* (Marcand *et al.* 2008) does not include the BAT domain, suggesting *RIF2* acquired this regulatory module after the duplication and divergence from *ORC4*. This functional BAT domain, which limits telomere elongation, may be a conserved feature of telomere length regulation; however it may be attached to different telomere proteins in different organisms. A regulatory motif with similar function to the BAT domain may be present on other proteins and may contribute to conservation of the telomere length equilibrium mechanism across species.

## Acknowledgments

We thank Brendan Cormack and Rebecca Keener for critical reading of the manuscript. This work was supported by National Institutes of Health 5R01GM043080 to C.W.G. and by support to the Johns Hopkins Telomere Center.

## Literature Cited

Armanios, M., and E. H. Blackburn, 2012 The telomere syndromes. Nat. Rev. Genet. 13: 693–704.

Ballew, B. J., and V. Lundblad, 2013 Multiple genetic pathways regulate replicative senescence in telomerase-deficient yeast. Aging Cell 12: 719–727.

Barnett, J. A., 2004 A history of research on yeasts 8: taxonomy. Yeast 21: 1141–1193.
Bianchi, A., and D. Shore, 2008 How telomerase reaches its end: mechanism of telomerase regulation by the telomeric complex. Mol. Cell 31: 153–165.
Bodnar, A. G., M. Ouellette, M. Frolkis, S. E. Holt, C. P. Chiu *et al.*, 1998 Extension of life-span by introduction of telomerase into normal human cells. Science 279: 349–352.
Bonetti, D., M. Clerici, S. Anbalagan, M. Martina, G. Lucchini *et al.*, 2010a Shelterin-like proteins and Yku inhibit nucleolytic processing of *Saccharomyces cerevisiae* telomeres. PLoS Genet. 6: e1000966.
Bonetti, D., M. Clerici, N. Manfrini, G. Lucchini, and M. P. Longhese, 2010b The MRX complex plays multiple functions in resection of Yku- and Rif2-protected DNA ends. PLoS One 5: e14142.
Brachmann, C. B., A. Davies, G. J. Cost, E. Caputo, J. Li *et al.*, 1998 Designer deletion strains derived from *Saccharomyces cerevisiae* S288C: a useful set of strains and plasmids for PCR-mediated gene disruption and other applications. Yeast 14: 115–132.
Buonomo, S. B., Y. Wu, D. Ferguson, and T. de Lange, 2009 Mammalian Rif1 contributes to replication stress survival and homology-directed repair. J. Cell Biol. 187: 385–398.
Byrne, K. P., and K. H. Wolfe, 2005 The Yeast Gene Order Browser: combining curated homology and syntenic context reveals gene fate in polyploid species. Genome Res. 15: 1456–1461.
Chang, M., J. C. Dittmar, and R. Rothstein, 2011 Long telomeres are preferentially extended during recombination-mediated telomere maintenance. Nat. Struct. Mol. Biol. 18: 451–456.
Colgin, L. M., K. Baran, P. Baumann, T. R. Cech, and R. R. Reddel, 2003 Human *POT1* facilitates telomere elongation by telomerase. Curr. Biol. 13: 942–946.
Cornacchia, D., V. Dileep, J. P. Quivy, R. Foti, F. Tili *et al.*, 2012 Mouse Rif1 is a key regulator of the replication-timing programme in mammalian cells. EMBO J. 31: 3678–3690.
d'Adda di Fagagna, F., P. M. Reaper, L. Clay-Farrace, H. Fiegler, P. Carr *et al.*, 2003 A DNA damage checkpoint response in telomere-initiated senescence. Nature 426: 194–198.
Di Virgilio, M., E. Callen, A. Yamane, W. Zhang, M. Jankovic *et al.*, 2013 Rif1 prevents resection of DNA breaks and promotes immunoglobulin class switching. Science 339: 711–715.
DuBois, M. L., Z. W. Haimberger, M. W. McIntosh, and D. E. Gottschling, 2002 A quantitative assay for telomere protection in *Saccharomyces cerevisiae*. Genetics 161: 995–1013.
Enomoto, S., L. Glowczewski, and J. Berman, 2002 *MEC3*, *MEC1*, and *DDC2* are essential components of a telomere checkpoint pathway required for cell cycle arrest during senescence in *Saccharomyces cerevisiae*. Mol. Biol. Cell 13: 2626–2638.
Escribano-Diaz, C., A. Orthwein, A. Fradet-Turcotte, M. Xing, J. T. Young *et al.*, 2013 A cell cycle-dependent regulatory circuit composed of *53BP1–RIF1* and BRCA1-CtIP controls DNA repair pathway choice. Mol. Cell 49: 872–883.
Gao, H., R. B. Cervantes, E. K. Mandell, J. H. Otero, and V. Lundblad, 2007 RPA-like proteins mediate yeast telomere function. Nat. Struct. Mol. Biol. 14: 208–214.
Gibson, D. G., 2011 Enzymatic assembly of overlapping DNA fragments. Methods Enzymol. 498: 349–361.
Grandin, N., S. I. Reed, and M. Charbonneau, 1997 Stn1, a new *Saccharomyces cerevisiae* protein, is implicated in telomere size regulation in association with Cdc13. Genes Dev. 11: 512–527.
Grandin, N., C. Damon, and M. Charbonneau, 2001 Ten1 functions in telomere end protection and length regulation in association with Stn1 and Cdc13. EMBO J. 20: 1173–1183.
Green, M., and J. Sambrook, 2012 *Molecular Cloning: A Laboratory Manual*. Cold Spring Harbor Laboratory Press, Cold Spring Harbor, NY.
Greider, C. W., and E. H. Blackburn, 1985 Identification of a specific telomere terminal transferase activity in *Tetrahymena* extracts. Cell 43: 405–413.
Hardy, C. F., L. Sussel, and D. Shore, 1992 A *RAP1*-interacting protein involved in transcriptional silencing and telomere length regulation. Genes Dev. 6: 801–814.
Harley, C. B., A. B. Futcher, and C. W. Greider, 1990 Telomeres shorten during ageing of human fibroblasts. Nature 345: 458–460.
Heidenreich, B., P. S. Rachakonda, K. Hemminki, and R. Kumar, 2014 TERT promoter mutations in cancer development. Curr. Opin. Genet. Dev. 24: 30–37.
Hirano, Y., K. Fukunaga, and K. Sugimoto, 2009 Rif1 and Rif2 inhibit localization of Tel1 to DNA ends. Mol. Cell 33: 312–322.
Horn, S., A. Figl, P. S. Rachakonda, C. Fischer, A. Sucker *et al.*, 2013 TERT promoter mutations in familial and sporadic melanoma. Science 339: 959–961.
Hu, Y., H. B. Tang, N. N. Liu, X. J. Tong, W. Dang *et al.*, 2013 Telomerase-null survivor screening identifies novel telomere recombination regulators. PLoS Genet. 9: e1003208.
Huang, F. W., E. Hodis, M. J. Xu, G. V. Kryukov, L. Chin *et al.*, 2013 Highly recurrent TERT promoter mutations in human melanoma. Science 339: 957–959.
IJpma, A., and C. W. Greider, 2003 Short telomeres induce a DNA damage response in *Saccharomyces cerevisiae*. Mol. Biol. Cell 14: 987–1001.
Kim, N. W., M. A. Piatyszek, K. R. Prowse, C. B. Harley, M. D. West *et al.*, 1994 Specific association of human telomerase activity with immortal cells and cancer. Science 266: 2011–2014.
Krauskopf, A., and E. H. Blackburn, 1996 Control of telomere growth by interactions of *RAP1* with the most distal telomeric repeats. Nature 383: 354–357.
Levy, D. L., and E. H. Blackburn, 2004 Counting of Rif1p and Rif2p on *Saccharomyces cerevisiae* telomeres regulates telomere length. Mol. Cell. Biol. 24: 10857–10867.
Lian, H. Y., E. D. Robertson, S. Hiraga, G. M. Alvino, D. Collingwood *et al.*, 2011 The effect of Ku on telomere replication time is mediated by telomere length but is independent of histone tail acetylation. Mol. Biol. Cell 22: 1753–1765.
Lin, J. J., and V. A. Zakian, 1996 The *Saccharomyces* Cdc13 protein is a single-strand TG1–3 telomeric DNA- binding protein in vitro that affects telomere behavior in vivo. Proc. Natl. Acad. Sci. USA 93: 13760–13765.
Lonergan, K. M., O. Iliopoulos, M. Ohh, T. Kamura, R. C. Conaway *et al.*, 1998 Regulation of hypoxia-inducible mRNAs by the von Hippel-Lindau tumor suppressor protein requires binding to complexes containing elongins B/C and Cul2. Mol. Cell. Biol. 18: 732–741.
Longtine, M., N. Wilson, M. Petracek, and J. Berman, 1989 A yeast telomere binding activity binds to two related telomere sequence motifs and is indistinguishable from *RAP1*. Curr. Genet. 16: 225–239.
Longtine, M. S., A. McKenzie, 3rd, D. J. Demarini, N. G. Shah, A. Wach *et al.*, 1998 Additional modules for versatile and economical PCR-based gene deletion and modification in *Saccharomyces cerevisiae*. Yeast 14: 953–961.
Lundblad, V., and J. W. Szostak, 1989 A mutant with a defect in telomere elongation leads to senescence in yeast. Cell 57: 633–643.
Ma, Y., and C. W. Greider, 2009 Kinase-independent functions of *TEL1* in telomere maintenance. Mol. Cell. Biol. 29: 5193–5202.
Marcand, S., E. Gilson, and D. Shore, 1997 A protein-counting mechanism for telomere length regulation in yeast. Science 275: 986–990.
Marcand, S., B. Pardo, A. Gratias, S. Cahun, and I. Callebaut, 2008 Multiple pathways inhibit NHEJ at telomeres. Genes Dev. 22: 1153–1158.

Mattarocci, S., M. Shyian, L. Lemmens, P. Damay, D. M. Altintas *et al.*, 2014 Rif1 controls DNA replication timing in yeast through the PP1 phosphatase Glc7. Cell Reports 7: 62–69.

Mosher, R. A., W. E. Durrant, D. Wang, J. Song, and X. Dong, 2006 A comprehensive structure-function analysis of Arabidopsis SNI1 defines essential regions and transcriptional repressor activity. Plant Cell 18: 1750–1765.

Nugent, C. I., T. R. Hughes, N. F. Lue, and V. Lundblad, 1996 Cdc13p: a single-strand telomeric DNA-binding protein with a dual role in yeast telomere maintenance. Science 274: 249–252.

Palm, W., and T. de Lange, 2008 How shelterin protects mammalian telomeres. Annu. Rev. Genet. 42: 301–334.

Peace, J. M., A. Ter-Zakarian, and O. M. Aparicio, 2014 Rif1 regulates initiation timing of late replication origins throughout the *S. cerevisiae* genome. PLoS One 9: e98501.

Schneider, C. A., W. S. Rasband, and K. W. Eliceiri, 2012 NIH Image to ImageJ: 25 years of image analysis. Nat. Methods 9: 671–675.

Shi, T., R. D. Bunker, S. Mattarocci, C. Ribeyre, M. Faty *et al.*, 2013 Rif1 and Rif2 shape telomere function and architecture through multivalent Rap1 interactions. Cell 153: 1340–1353.

Shore, D., and A. Bianchi, 2009 Telomere length regulation: coupling DNA end processing to feedback regulation of telomerase. EMBO J. 28: 2309–2322.

Sikorski, R. S., and P. Hieter, 1989 A system of shuttle vectors and yeast host strains designed for efficient manipulation of DNA in *Saccharomyces cerevisiae*. Genetics 122: 19–27.

Smith, C. D., D. L. Smith, J. L. DeRisi, and E. H. Blackburn, 2003 Telomeric protein distributions and remodeling through the cell cycle in *Saccharomyces cerevisiae*. Mol. Biol. Cell 14: 556–570.

Smith, S., and T. de Lange, 2000 Tankyrase promotes telomere elongation in human cells. Curr. Biol. 10: 1299–1302.

Smogorzewska, A., and T. de Lange, 2004 Regulation of telomerase by telomeric proteins. Annu. Rev. Biochem. 73: 177–208.

Teng, S., J. Chang, B. McCowan, and V. A. Zakian, 2000 Telomerase-independent lengthening of yeast telomeres occurs by an abrupt Rad50p-dependent, Rif-inhibited recombinational process. Mol. Cell 6: 947–952.

van Steensel, B., and T. de Lange, 1997 Control of telomere length by the human telomeric protein TRF1. Nature 385: 740–743.

Veldman, T., K. T. Etheridge, and C. M. Counter, 2004 Loss of hPot1 function leads to telomere instability and a cut-like phenotype. Curr. Biol. 14: 2264–2270.

Viggiani, C. J., and O. M. Aparicio, 2006 New vectors for simplified construction of BrdU-Incorporating strains of *Saccharomyces cerevisiae*. Yeast 23: 1045–1051.

Wellinger, R. J., and V. A. Zakian, 2012 Everything you ever wanted to know about *Saccharomyces cerevisiae* telomeres: beginning to end. Genetics 191: 1073–1105.

Wotton, D., and D. Shore, 1997 A novel Rap1p-interacting factor, Rif2p, cooperates with Rif1p to regulate telomere length in *Saccharomyces cerevisiae*. Genes Dev. 11: 748–760.

Yamazaki, S., A. Ishii, Y. Kanoh, M. Oda, Y. Nishito *et al.*, 2012 Rif1 regulates the replication timing domains on the human genome. EMBO J. 31: 3667–3677.

Zimmermann, M., F. Lottersberger, S. B. Buonomo, A. Sfeir, and T. de Lange, 2013 53BP1 regulates DSB repair using Rif1 to control 5′ end resection. Science 339: 700–704.

*Communicating editor: N. Hollingsworth*

GENETICS

**Supporting Information**
www.genetics.org/lookup/suppl/doi:10.1534/genetics.115.177899/-/DC1

# Regulation of Telomere Length Requires a Conserved N-Terminal Domain of Rif2 in *Saccharomyces cerevisiae*

**Hannah Kaizer, Carla J. Connelly, Kelsey Bettridge, Christopher Viggiani, and Carol W. Greider**


DOI: 10.1534/genetics.115.177899

# Supporting Information

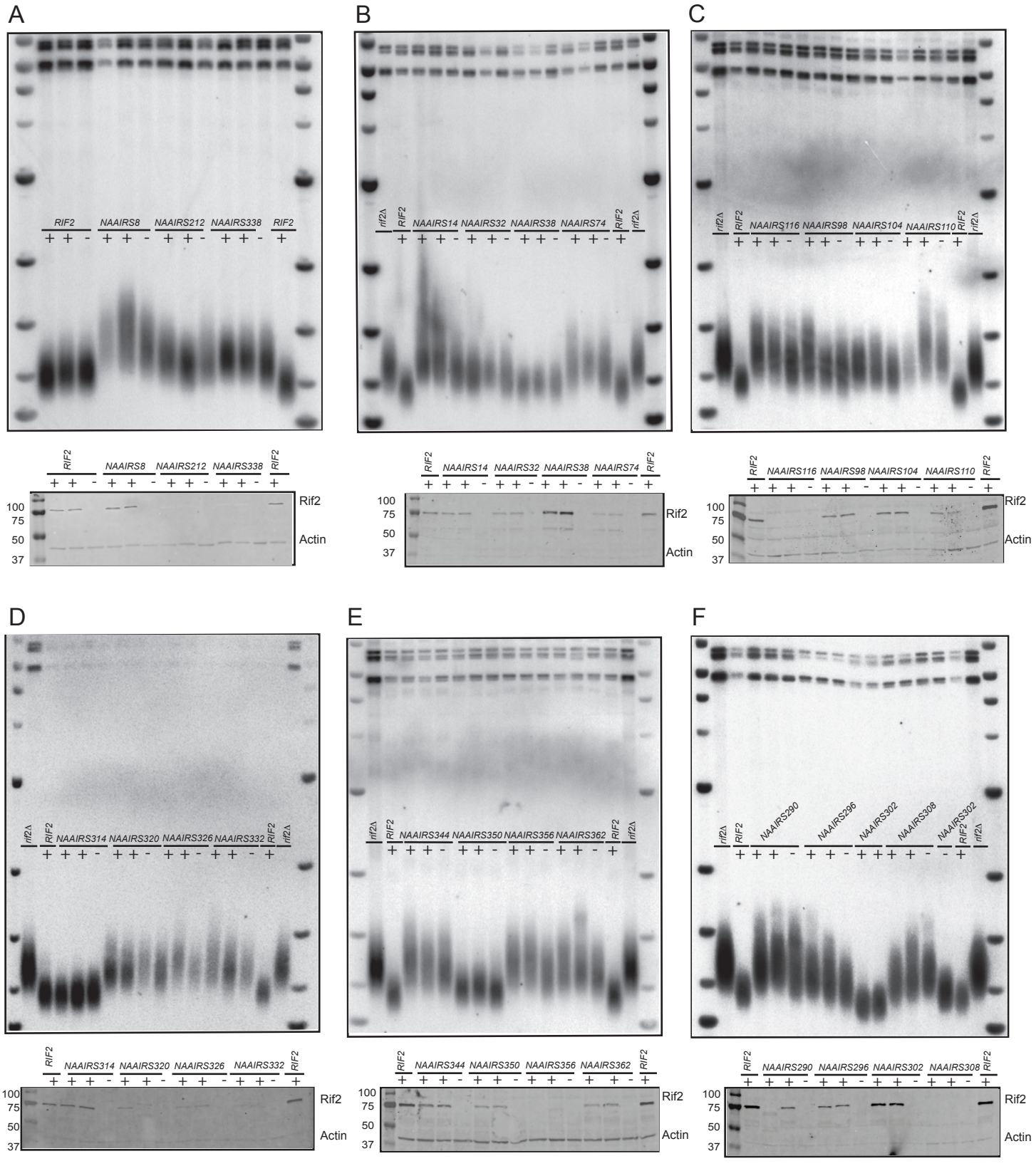


**Figure S1. NAAIRS scanning mutagenesis identifies functional regions of *RIF2*.** (A)-(F) The original Southern blots (Top) and western (bottom) for the NAAIRS screen are shown. In each gel two independent13xMyc tagged haploids are shown (+) and one untagged control of the same mutant (-). The Rif2-13xMyc tagged protein level was normalized to the actin loading control as described in the materials and methods. When discrepancies were found between independent transformants additional independent transformants were examined to determine the phenotype. The mutants were assayed as they were sequence verified, and thus the mutants are not in numerical order on these preliminary gels.

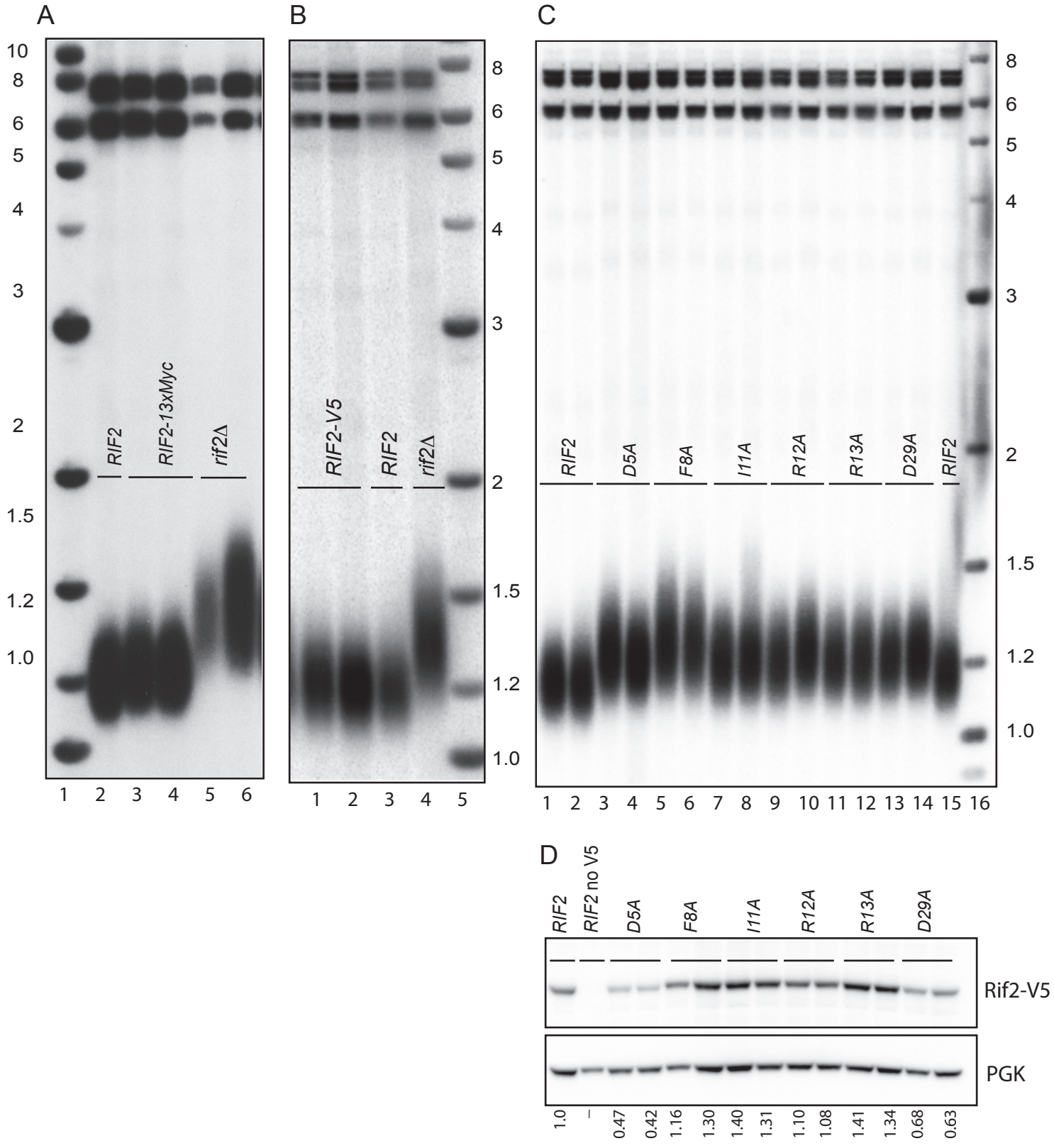


**Figure S2. Tagging of *RIF2* does not disrupt function**. (A) The telomere length in the wild type 13xMyc tagged *RIF2* strains are similar to the untagged wild type strain. (B) The telomere length in the V5 tagged *RIF2* integrated at the endogenous *RIF2* locus is similar to wild type. (C) Single amino acid mutations that show long telomeres were retested for protein telomere length and (D) for Rif2 protein expression level. The numbers below represent quantification of Rif2 levels, normalized to the PGK loading control, and then to the wild type *RIF2* (See Materials and Methods).

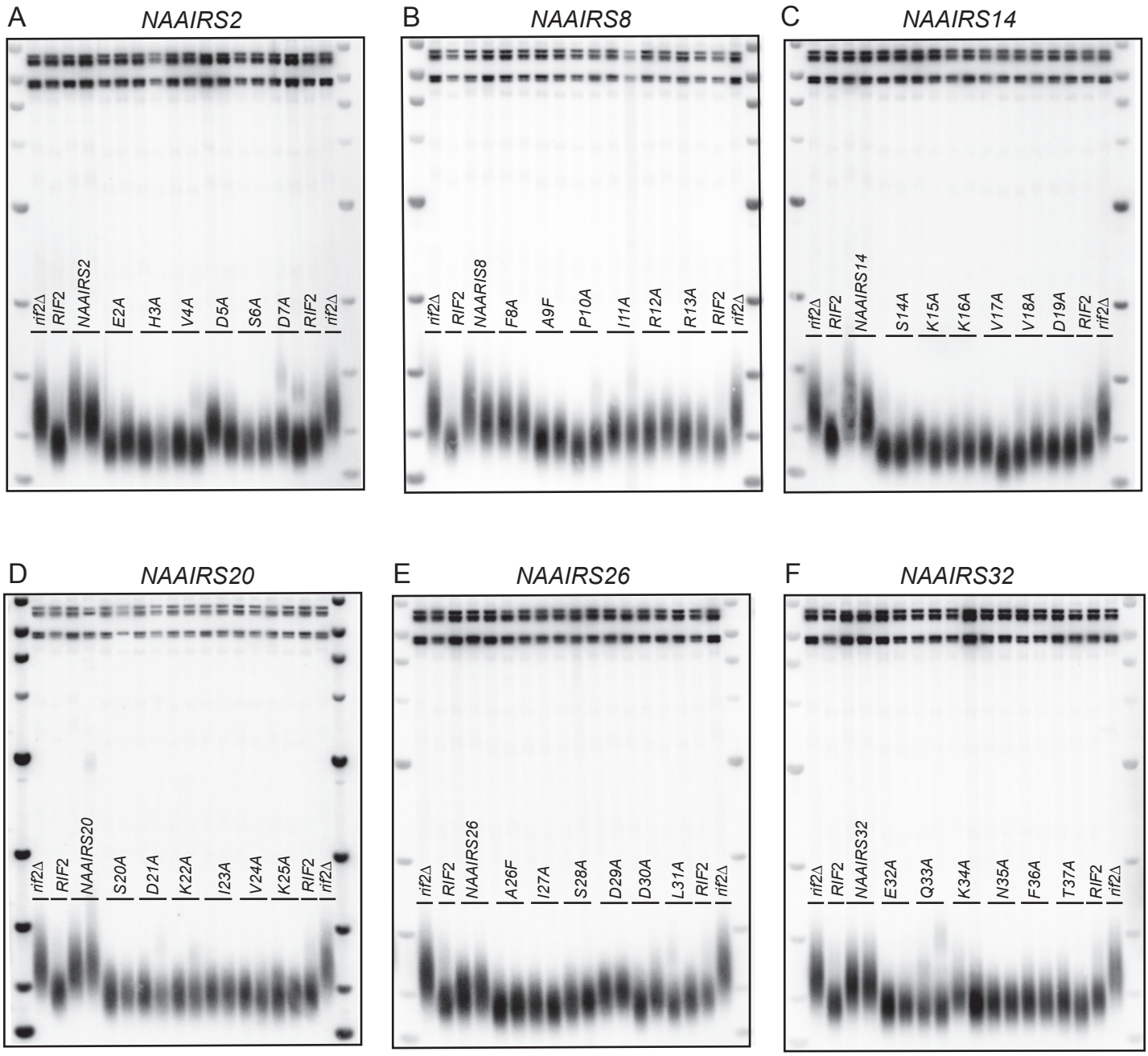


**Figure S3. Individual single amino acid changes across Rif2 N-terminus.** (A)-(F). Each amino acid across the six N-terminal NAAIRS mutants: *rif2-NAAIRS2*, *rif2-NAAIRS8*, *rif2-NAAIRS14*, *rif2-NAAIRS20*, *rif2-NAAIRS26*, and *rif2-NAAIRS32* were individually mutated and telomere length was measured and compared to *rif2*Δ and *RIF2* telomere length on the same gel. For each amino acid change two independent transformants were measured.

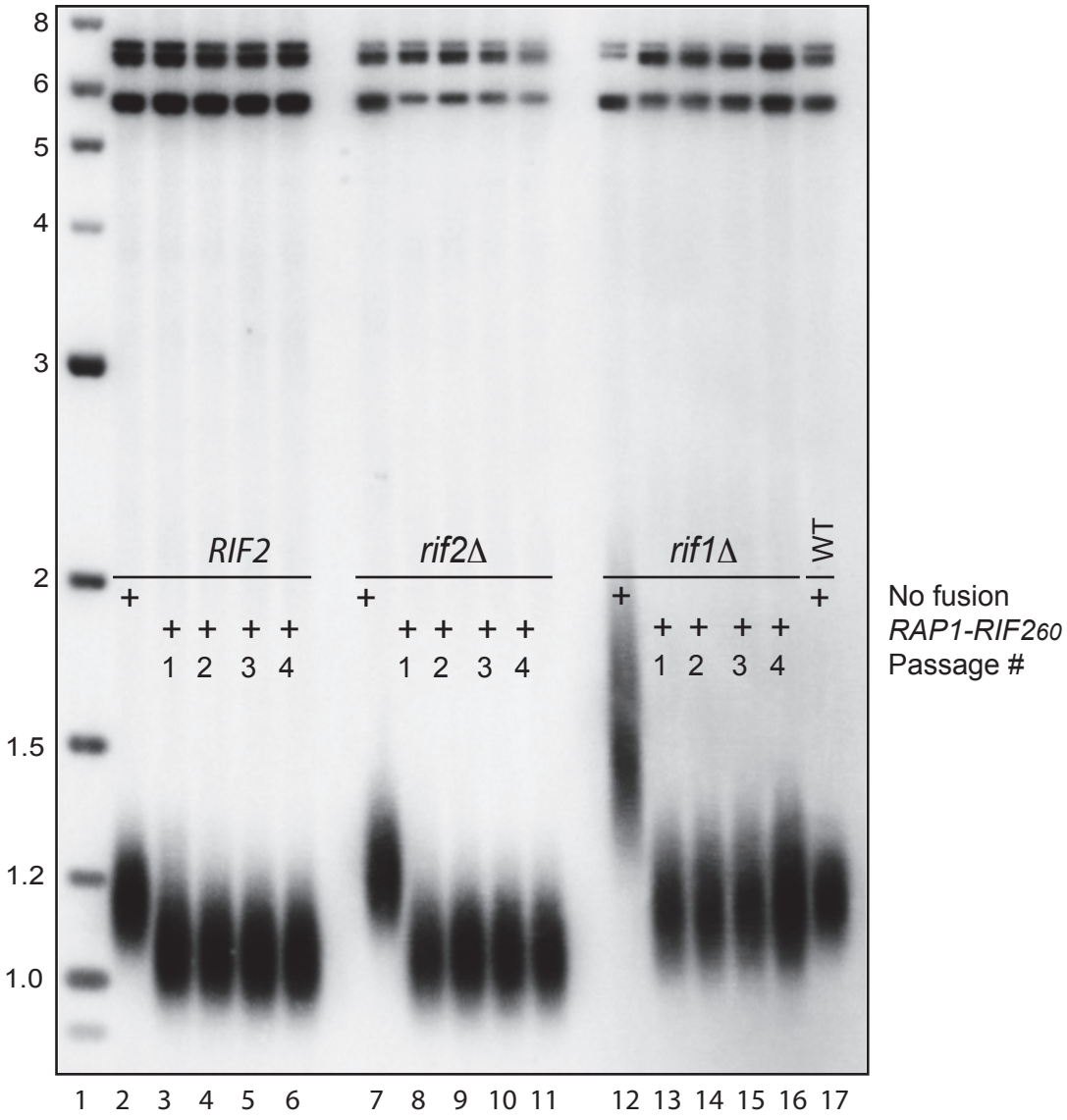


**Figure S4**. **Telomere length during passaging of cells expressing of *RAP1-RIF2$_{60}$ fusion***. Haploid segregants of *RIF2*, *rif2*Δ, or *rif1*Δ mutants containing *RAP1-RIF2*$_{60}$ were grown for 4 consecutive passages in YPD broth. Telomere length at each passage was analyzed. The size markers on the side represent kb.

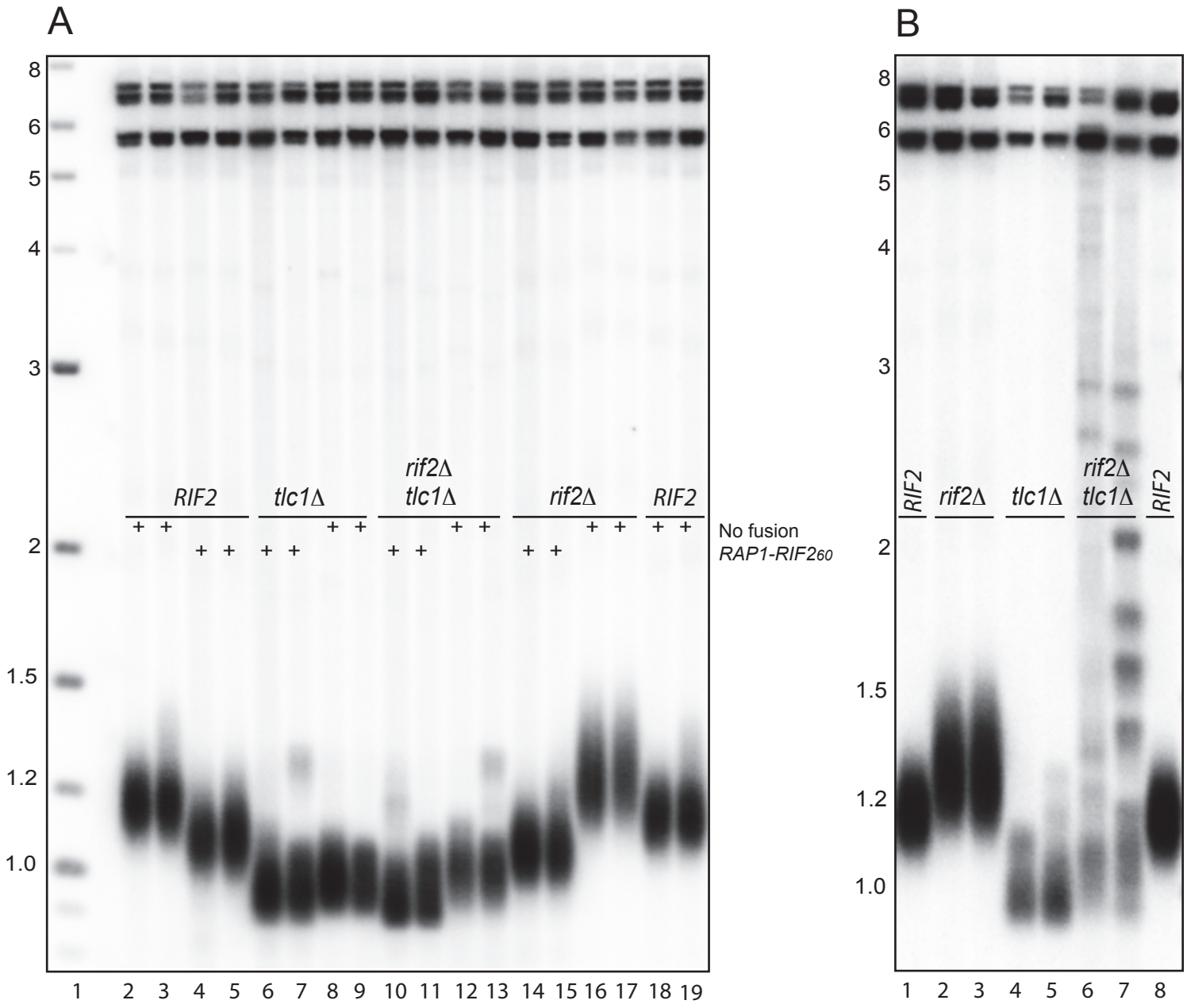


**Figure S5. Telomerase is epistatic to RAP1-RIF260 fusion** (A) Southern blot telomere analysis of *RIF2*, *rif2*Δ *tlc1*Δ, and *rif2*Δ *tlc1*Δ cells expressing the *RAP1-RIF2*$_{60}$ or no fusion protein. The genotype of the strain is indicated above each lane and the presence or absence of the fusion protein is shown with a + sign. (B) Southern blot telomere analysis of *RIF2 RIF1*, *rif2*Δ, *tlc1*Δ, and *rif2*Δ *tlc1*Δ cells grown for additional generations. The higher bands that appear between 1-3 kb in the *rif2*Δ *tlc1*Δ cells represent the early emergence of telomerase null survivors (Chang et al. 2011; Ballew and Lundblad 2013; Hu et al. 2013). The shortest telomeres are longer in these *rif2*Δ *tlc1*Δ survivors. The size markers on the side represent kb

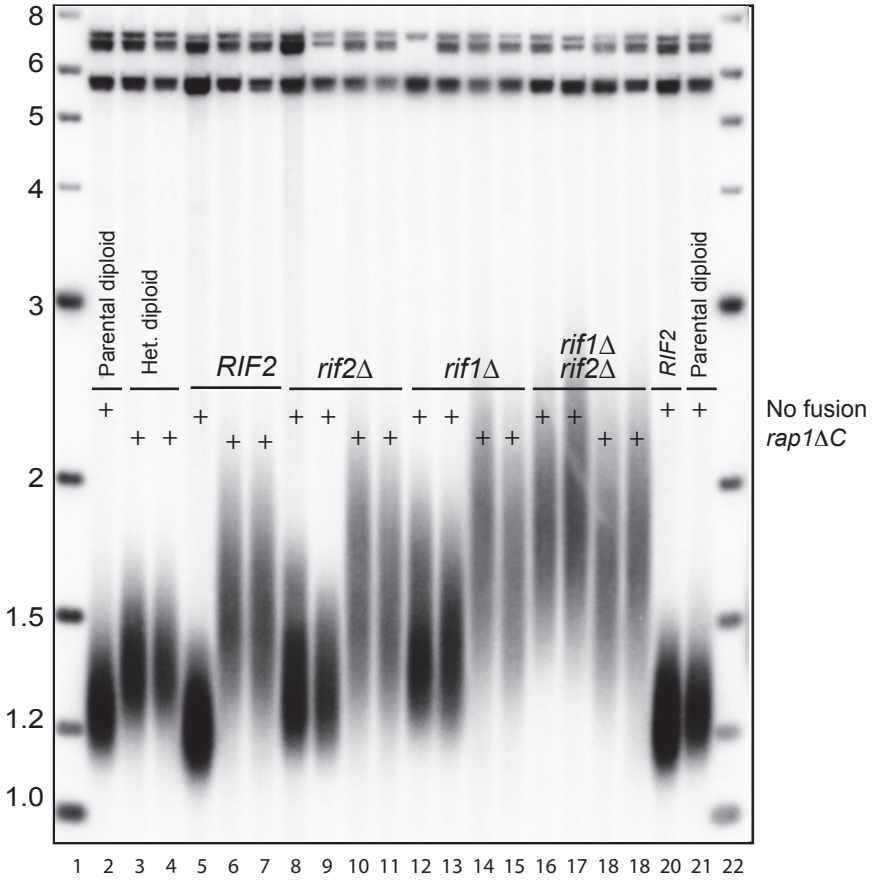


**Figure S6. Expression of *Rap1ΔC* without the BAT domain does not rescue telomere length.** A *rap1ΔC* truncation without the Rif260 BAT domain was expressed in in *rif1*Δ, *rif2*Δ, and *rif1*Δ *rif2*Δ cells and Southern blot telomere analysis was carried out. The genotype of the strain is indicated above each lane and the presence or absence of *rap1*ΔC truncation is shown with a + sign. The parental diploid was transformed with the fusion construct to yield the heterozyous diploid (Het. diploid) and was dissected for the haploid segregants. The size markers on the side represent kb.

**Table S1 Yeast Strains 1: *rif2NAAIRS* mutants integrated at the *URA3* locus**

| Strain | Genotype | Source |
|---|---|---|
| OAy1002 | *MAT**a** ade2-1 trp1-1 ura3-1 leu2-3,112 his3-11,15 can1-100 RAD5* | Viggiani and Aparicio (2006) |
| OAy1003 | *MATα ade2-1 trp1-1 ura3-1 leu2-3,112 his3-11,15 can1-100 RAD5* | Viggiani and Aparicio (2006) |
| CVy242 | *MAT**a**/MATα ade2-1/ade2-1 trp1-1/trp1-1 ura3-1/ura3-1 leu2-3,112/leu2-3,112 his3-11,15/his3-11,15 can1-100/can1-100 RAD5/RAD5* | This study |
| CVy245 | *MAT**a**/MATα ade2-1/ade2-1 trp1-1/trp1-1 ura3-1/ura3-1 leu2-3,112/leu2-3,112 his3-11,15/his3-11,15 can1-100/can1-100 RAD5/RAD5 RIF2/rif2Δ::kanMX4* | This study |
| CVy275 | CVy245 *ura3-1/ura3-1*::(*RIF2-URA3*) | This study |
| HKy295, 296 | CVy245 *ura3-1/ura3-1*::(*rif2NAAIRS2-URA3*) | This study |
| HKy297, 298 | CVy245 *ura3-1/ura3-1*::(*rif2NAAIRS8-URA3*) | This study |
| HKy299, 300 | CVy245 *ura3-1/ura3-1*::(*rif2NAAIRS14-URA3*) | This study |
| HKy342, 343 | CVy245 *ura3-1/ura3-1*::(*rif2NAAIRS20-URA3*) | This study |
| HKy344, 345 | CVy245 *ura3-1/ura3-1*::(*rif2NAAIRS26-URA3*) | This study |
| HKy301, 302 | CVy245 *ura3-1/ura3-1*::(*rif2NAAIRS32-URA3*) | This study |
| HKy303, 304 | CVy245 *ura3-1/ura3-1*::(*rif2NAAIRS38-URA3*) | This study |
| HKy346, 347 | CVy245 *ura3-1/ura3-1*::(*rif2NAAIRS44-URA3*) | This study |
| KGy155 A, B | CVy245 *ura3-1/ura3-1*::(*rif2NAAIRS50-URA3*) | This study |
| KGy107 A, B | CVy245 *ura3-1/ura3-1*::(*rif2NAAIRS56-URA3*) | This study |
| KGy108 A, B | CVy245 *ura3-1/ura3-1*::(*rif2NAAIRS62-URA3*) | This study |
| KGy109 A, B | CVy245 *ura3-1/ura3-1*::(*rif2NAAIRS68-URA3*) | This study |
| HKy305, 306 | CVy245 *ura3-1/ura3-1*::(*rif2NAAIRS74-URA3*) | This study |
| HKy348, 349 | CVy245 *ura3-1/ura3-1*::(*rif2NAAIRS80-URA3*) | This study |
| HKy350, 351 | CVy245 *ura3-1/ura3-1*::(*rif2NAAIRS86-URA3*) | This study |
| HKy352, 353 | CVy245 *ura3-1/ura3-1*::(*rif2NAAIRS92-URA3*) | This study |
| HKy354, 355 | CVy245 *ura3-1/ura3-1*::(*rif2NAAIRS98-URA3*) | This study |
| HKy356, 357 | CVy245 *ura3-1/ura3-1*::(*rif2NAAIRS104-URA3*) | This study |
| HKy358, 359 | CVy245 *ura3-1/ura3-1*::(*rif2NAAIRS110-URA3*) | This study |
| HKy307, 308 | CVy245 *ura3-1/ura3-1*::(*rif2NAAIRS116-URA3*) | This study |
| HKy309, 310 | CVy245 *ura3-1/ura3-1*::(*rif2NAAIRS122-URA3*) | This study |
| HKy311, 312 | CVy245 *ura3-1/ura3-1*::(*rif2NAAIRS128-URA3*) | This study |
| KGy120A, B | CVy245 *ura3-1/ura3-1*::(*rif2NAAIRS134-URA3*) | This study |
| HKy314, 315 | CVy245 *ura3-1/ura3-1*::(*rif2NAAIRS140-URA3*) | This study |
| KGy122A, B | CVy245 *ura3-1/ura3-1*::(*rif2NAAIRS146-URA3*) | This study |
| KGy123A, B | CVy245 *ura3-1/ura3-1*::(*rif2NAAIRS152-URA3*) | This study |
| KGy156A, B | CVy245 *ura3-1/ura3-1*::(*rif2NAAIRS158-URA3*) | This study |
| KGy124A, B | CVy245 *ura3-1/ura3-1*::(*rif2NAAIRS164-URA3*) | This study |
| KGy125A, B | CVy245 *ura3-1/ura3-1*::(*rif2NAAIRS170-URA3*) | This study |
| KGy126A, B | CVy245 *ura3-1/ura3-1*::(*rif2NAAIRS182-URA3*) | This study |
| KGy127A, B | CVy245 *ura3-1/ura3-1*::(*rif2NAAIRS188-URA3*) | This study |
| HKy316, 317 | CVy245 *ura3-1/ura3-1*::(*rif2NAAIRS194-URA3*) | This study |
| HKy318, 319 | CVy245 *ura3-1/ura3-1*::(*rif2NAAIRS200-URA3*) | This study |

Table S1, *continued*

| Strain | Genotype | Source |
|---|---|---|
| HKy320, 321 | CVy245 *ura3-1/ura3-1*::(*rif2NAAIRS206-URA3*) | This study |
| HKy322, 323 | CVy245 *ura3-1/ura3-1*::(*rif2NAAIRS212-URA3*) | This study |
| KGy132A, B | CVy245 *ura3-1/ura3-1*::(*rif2NAAIRS218-URA3*) | This study |
| HKy324, 325 | CVy245 *ura3-1/ura3-1*::(*rif2NAAIRS230-URA3*) | This study |
| HKy326, 327 | CVy245 *ura3-1/ura3-1*::(*rif2NAAIRS236-URA3*) | This study |
| HKy328, 329 | CVy245 *ura3-1/ura3-1*::(*rif2NAAIRS242-URA3*) | This study |
| HKy330, 331 | CVy245 *ura3-1/ura3-1*::(*rif2NAAIRS248-URA3*) | This study |
| KGy137A, B | CVy245 *ura3-1/ura3-1*::(*rif2NAAIRS260-URA3*) | This study |
| KGy138A, B | CVy245 *ura3-1/ura3-1*::(*rif2NAAIRS266-URA3*) | This study |
| HKy360, 361 | CVy245 *ura3-1/ura3-1*::(*rif2NAAIRS272-URA3*) | This study |
| KGy139A, B | CVy245 *ura3-1/ura3-1*::(*rif2NAAIRS278-URA3*) | This study |
| KGy140A, B | CVy245 *ura3-1/ura3-1*::(*rif2NAAIRS284-URA3*) | This study |
| HKy362, 363 | CVy245 *ura3-1/ura3-1*::(*rif2NAAIRS290-URA3*) | This study |
| HKy364, 365 | CVy245 *ura3-1/ura3-1*::(*rif2NAAIRS296-URA3*) | This study |
| HKy366, 367 | CVy245 *ura3-1/ura3-1*::(*rif2NAAIRS302-URA3*) | This study |
| HKy368, 369 | CVy245 *ura3-1/ura3-1*::(*rif2NAAIRS308-URA3*) | This study |
| HKy370, 371 | CVy245 *ura3-1/ura3-1*::(*rif2NAAIRS314-URA3*) | This study |
| HKy372, 373 | CVy245 *ura3-1/ura3-1*::(*rif2NAAIRS320-URA3*) | This study |
| HKy332, 333 | CVy245 *ura3-1/ura3-1*::(*rif2NAAIRS326-URA3*) | This study |
| HKy334, 335 | CVy245 *ura3-1/ura3-1*::(*rif2NAAIRS332-URA3*) | This study |
| HKy336, 337 | CVy245 *ura3-1/ura3-1*::(*rif2NAAIRS338-URA3*) | This study |
| HKy338, 339 | CVy245 *ura3-1/ura3-1*::(*rif2NAAIRS344-URA3*) | This study |
| HKy340, 341 | CVy245 *ura3-1/ura3-1*::(*rif2NAAIRS350-URA3*) | This study |
| HKy374, 375 | CVy245 *ura3-1/ura3-1*::(*rif2NAAIRS356-URA3*) | This study |
| HKy376, 377 | CVy245 *ura3-1/ura3-1*::(*rif2NAAIRS362-URA3*) | This study |
| HKy378, 379 | CVy245 *ura3-1/ura3-1*::(*rif2NAAIRS368-URA3*) | This study |
| HKy382, 383 | CVy245 *ura3-1/ura3-1*::(*rif2NAAIRS374-URA3*) | This study |
| KGy147A, B | CVy245 *ura3-1/ura3-1*::(*rif2NAAIRS380-URA3*) | This study |
| HKy380-381 | CVy245 *ura3-1/ura3-1*::(*rif2NAAIRS386-URA3*) | This study |
| KGy148A, B | CVy245 *ura3-1/ura3-1*::(*rif2NAAIRS392-URA3*) | This study |

**Table S1 Yeast strain 1: *rif2 NAAIRS* mutants integrated at the *URA3* locus**
The diploid yeast strains for NAAIRS176, 224, and 254 integrated at the URA3 locus were inadvertently not saved, however, all the other strains and the haploid segregants for all of the NAAIRS mutants are available upon request.

**Table S2 Yeast Strains 2: Epitope-tagged *rif2* mutants**

| Strain | Genotype | Source |
|---|---|---|
| KGy149, 151 | *MATα ade2-1 trp1-1 ura3-1 leu2-3,112 his3-11,15 can1-100 RAD5 ura3-1*::(*RIF2-URA3*) | This study |
| HKy385, 386 | KGy149 *ura3-1::(RIF2-13Myc-URA3)* | This study |
| HKy393, 394 | KGy149 *ura3-1::(rif2NAAIRS2-13Myc-URA3)* | This study |
| HKy387, 388 | KGy149 *ura3-1::(rif2NAAIRS8-13Myc-URA3)* | This study |
| HKy401, 402 | KGy149 *ura3-1::(rif2NAAIRS14-13Myc-URA3)* | This study |
| HKy405, 406 | KGy149 *ura3-1::(rif2NAAIRS20-13Myc-URA3)* | This study |
| HKy407, 408 | KGy149 *ura3-1::(rif2NAAIRS26-13Myc-URA3)* | This study |
| HKy395, 396 | KGy149 *ura3-1::(rif2NAAIRS32-13Myc-URA3)* | This study |
| HKy409, 410 | KGy149 *ura3-1::(rif2NAAIRS44-13Myc-URA3)* | This study |
| HKy403, 404 | KGy149 *ura3-1::(rif2NAAIRS74-13Myc-URA3)* | This study |
| HKy435, 436 | KGy149 *ura3-1::(rif2NAAIRS80-13Myc-URA3)* | This study |
| HKy437, 438 | KGy149 *ura3-1::(rif2NAAIRS86-13Myc-URA3)* | This study |
| HKy411, 412 | KGy149 *ura3-1::(rif2NAAIRS98-13Myc-URA3)* | This study |
| HKy413, 414 | KGy149 *ura3-1::(rif2NAAIRS104-13Myc-URA3)* | This study |
| HKy415, 416 | KGy149 *ura3-1::(rif2NAAIRS110-13Myc-URA3)* | This study |
| HKy397, 398 | KGy149 *ura3-1::(rif2NAAIRS116-13Myc-URA3)* | This study |
| HKy439, 440 | KGy149 *ura3-1::(rif2NAAIRS122-13Myc-URA3)* | This study |
| HKy441, 442 | KGy149 *ura3-1::(rif2NAAIRS128-13Myc-URA3)* | This study |
| HKy451, 452 | KGy149 *ura3-1::(rif2NAAIRS140-13Myc-URA3)* | This study |
| HKy453, 454 | KGy149 *ura3-1::(rif2NAAIRS194-13Myc-URA3)* | This study |
| HKy399, 400 | KGy149 *ura3-1::(rif2NAAIRS206-13Myc-URA3)* | This study |
| HKy389, 390 | KGy149 *ura3-1::(rif2NAAIRS212-13Myc-URA3)* | This study |
| HKy417, 418 | KGy149 *ura3-1::(rif2NAAIRS230-13Myc-URA3)* | This study |
| HKy419, 420 | KGy149 *ura3-1::(rif2NAAIRS236-13Myc-URA3)* | This study |
| HKy421, 422 | KGy149 *ura3-1::(rif2NAAIRS242-13Myc-URA3)* | This study |
| HKy423, 424 | KGy149 *ura3-1::(rif2NAAIRS248-13Myc-URA3)* | This study |
| HKy462, 463 | KGy149 *ura3-1::(rif2NAAIRS290-13Myc-URA3)* | This study |
| HKy425, 426 | KGy149 *ura3-1::(rif2NAAIRS296-13Myc-URA3)* | This study |
| Hky427, 428 | KGy149 *ura3-1::(rif2NAAIRS302-13Myc-URA3)* | This study |
| HKy464, 465 | KGy149 *ura3-1::(rif2NAAIRS308-13Myc-URA3)* | This study |
| HKy443, 444 | KGy149 *ura3-1::(rif2NAAIRS314-13Myc-URA3)* | This study |
| HKy445, 446 | KGy149 *ura3-1::(rif2NAAIRS320-13Myc-URA3)* | This study |
| HKy447, 448 | KGy149 *ura3-1::(rif2NAAIRS326-13Myc-URA3)* | This study |
| HKy449, 450 | KGy149 *ura3-1::(rif2NAAIRS332-13Myc-URA3)* | This study |
| HKy391, 392 | KGy149 *ura3-1::(rif2NAAIRS338-13Myc-URA3)* | This study |
| HKy429, 430 | KGy149 *ura3-1::(rif2NAAIRS344-13Myc-URA3)* | This study |
| HKy431, 432 | KGy149 *ura3-1::(rif2NAAIRS350-13Myc-URA3)* | This study |
| HKy458, 459 | KGy149 *ura3-1::(rif2NAAIRS356-13Myc-URA3)* | This study |
| HKy433, 434 | KGy149 *ura3-1::(rif2NAAIRS362-13Myc-URA3)* | This study |
| HKy460, 461 | KGy149 *ura3-1::(rif2NAAIRS368-13Myc-URA3)* | This study |

Table S2, *continued*

| Strain | Genotype | Source |
|---|---|---|
| HKy374 | KGy149 *ura3-1::(rif2NAAIRS374-13Myc-URA3)* | This study |
| HKy455, 456 | KGy149 *ura3-1::(rif2NAAIRS386-13Myc-URA3)* | This study |
| HKy466, 467 | *MATα ade2-1 trp1-1 ura3-1 leu2-3,112 his3-11,15 can1-100 RAD5* | Dissection CVy245 |
| HKy468, 469 | *MATα ade2-1 trp1-1 ura3-1 leu2-3,112 his3-11,15 can1-100 RAD5 rif2Δ::kanMX4* | Dissection CVy245 |
| HKy470, 471 | OAy1002 *RIF2-V5-URA3* | This study |
| HKy472, 473 | OAy1002 *rif2(S28A)-V5-URA3* | This study |
| HKy474, 475 | OAy1002 *rif2(Y122A)-V5-URA3* | This study |
| HKy476, 477 | OAy1002 *rif2(G124A)-V5-URA3* | This study |
| HKy478, 479 | OAy1002 *rif2(I125A)-V5-URA3* | This study |
| HKy480, 481 | OAy1002 *rif2(R127A)-V5-URA3* | This study |
| HKy482, 483 | OAy1002 *rif2(D126A)-V5-URA3* | This study |
| HKy498, 499 | OAy1002 *rif2(L39A)-V5-URA3* | This study |
| HKy500, 501 | OAy1002 *rif2(R40A)-V5-URA3* | This study |
| HKy502, 503 | OAy1002 *rif2(K41A)-V5-URA3* | This study |
| HKy504, 505 | OAy1002 *rif2(V38A)-V5-URA3* | This study |
| HKy506, 507 | OAy1002 *rif2(L47A)-V5-URA3* | This study |
| HKy508, 509 | OAy1002 *rif2(K269A)-V5-URA3* | This study |
| HKy510, 511 | OAy1002 *rif2(N43A)-V5-URA3* | This study |
| HKy512, 513 | OAy1002 *rif2(I233A)-V5-URA3* | This study |
| HKy514, 515 | OAy1002 *rif2(L44A)-V5-URA3* | This study |
| HKy516, 517 | OAy1002 *rif2(H120A)-V5-URA3* | This study |
| HKy518, 519 | OAy1002 *rif2(I233C)-V5-URA3* | This study |
| HKy520, 521 | OAy1002 *rif2(F8A)-V5-URA3* | This study |
| HKy522, 523 | OAy1002 *rif2(A9F)-V5-URA3* | This study |
| HKy524, 525 | OAy1002 *rif2(P10A)-V5-URA3* | This study |
| HKy526, 527 | OAy1002 *rif2(I11A)-V5-URA3* | This study |
| HKy528, 529 | OAy1002 *rif2(R12A)-V5-URA3* | This study |
| HKy531, 532 | OAy1002 *rif2(R13A)-V5-URA3* | This study |
| HKy538, 539 | OAy1002 *rif2(S14A)-V5-URA3* | This study |
| HKy540, 541 | OAy1002 *rif2(K15A)-V5-URA3* | This study |
| HKy542, 543 | OAy1002 *rif2(K16A)-V5-URA3* | This study |
| HKy549, 550 | OAy1002 *rif2(V17A)-V5-URA3* | This study |
| HKy544, 545 | OAy1002 *rif2(V18A)-V5-URA3* | This study |
| HKy546, 547 | OAy1002 *rif2(D19A)-V5-URA3* | This study |
| HKy555, 556 | OAy1002 *rif2(S20A)-V5-URA3* | This study |
| HKy557, 558 | OAy1002 *rif2(D21A)-V5-URA3* | This study |
| HKy559, 560 | OAy1002 *rif2(K22A)-V5-URA3* | This study |
| HKy561, 562 | OAy1002 *rif2(I23A)-V5-URA3* | This study |
| HKy563, 564 | OAy1002 *rif2(V24A)-V5-URA3* | This study |
| HKy565, 566 | OAy1002 *rif2(K25A)-V5-URA3* | This study |
| HKy567, 568 | OAy1002 *rif2(V45A)-V5-URA3* | This study |
| HKy659, 570 | OAy1002 *rif2(P46A)-V5-URA3* | This study |

Table S2, *continued*

| Strain | Genotype | Source |
|---|---|---|
| HKy571, 572 | OAy1002 *rif2(I47A)-V5-URA3* | This study |
| HKy573, 574 | OAy1002 *rif2(K48A)-V5-URA3* | This study |
| HKy575, 576 | OAy1002 *rif2(K49A)-V5-URA3* | This study |
| HKy577, 578 | OAy1002 *rif2(E2A)-V5-URA3* | This study |
| HKy579, 580 | OAy1002 *rif2(H3A)-V5-URA3* | This study |
| HKy581, 582 | OAy1002 *rif2(V4A)-V5-URA3* | This study |
| HKy583, 584 | OAy1002 *rif2(D5A)-V5-URA3* | This study |
| HKy585, 586 | OAy1002 *rif2(S6A)-V5-URA3* | This study |
| HKy587, 588 | OAy1002 *rif2(D7A)-V5-URA3* | This study |
| HKy589, 590 | OAy1002 *rif2(A26F)-V5-URA3* | This study |
| HKy591, 592 | OAy1002 *rif2(I27A)-V5-URA3* | This study |
| HKy593, 594 | OAy1002 *rif2(D29A)-V5-URA3* | This study |
| HKy595, 596 | OAy1002 *rif2(D30A)-V5-URA3* | This study |
| HKy597, 598 | OAy1002 *rif2(L31A)-V5-URA3* | This study |
| HKy599, 600 | OAy1002 *rif2(E32A)-V5-URA3* | This study |
| HKy601, 602 | OAy1002 *rif2(Q33A)-V5-URA3* | This study |
| HKy603, 604 | OAy1002 *rif2(K34A)-V5-URA3* | This study |
| HKy605, 606 | OAy1002 *rif2(N35A)-V5-URA3* | This study |
| HKy607, 608 | OAy1002 *rif2(F36A)-V5-URA3* | This study |
| HKy609, 610 | OAy1002 *rif2(T37A)-V5-URA3* | This study |
| HKy548 | OAy1002 *rif2Δ::KanMX4* | This study |

**Table S3 Yeast Strains 3: *RAP1-RIF2* fusions integrated at the *RAP1* locus**

| Strain | Genotype | Source |
|---|---|---|
| HKy551, 552 | CVy242 *RIF2/rif2Δ::kanMX4 RAP1/rap1*::(*RAP1-RIF2$_{60}$-URA3*) | This study |
| HKy621, 622 | CVy242 *RIF2/rif2Δ::kanMX4 RIF1/rif1Δ::LEU2 RAP1/rap1::(RAP1-RIF2$_{60}$-URA3)* | This study |
| HKy639 | CVy242 *RIF2/rif2Δ::kanMX4 RIF1/rif1Δ::LEU2* | This study |
| HKy662, 663 | HKy639 *RAP1/rap1::(RAP1-rif2$_{60}$ [F8A]-URA3)* | This study |
| HKy782, 783 | HKy639 *RAP1/rap1::(RAP1-rif2$_{60}$ [F8W]-URA3)* | This study |
| HKy796, 797 | HKy639 *RAP1/rap1::(RAP1-rif2$_{60}$ [F8Y]-URA3)* | This study |
| HKy768, 769 | HKy639 *RAP1/rap1::(rap1ΔC-RIF2$_{60}$-URA3)* | This study |
| HKy754, 755 | HKy639 *RAP1*/rap1*::(rap1ΔC-URA3)* | This study |
| HKy736, 737 | HKy639 *RAP1/rap1::(RAP1-RIF2$_{36}$-URA3)* | This study |
| YCC115 | *MAT**a**/MATα his3Δ1/his3Δ1 leu2Δ0/leu2Δ0 lys2Δ0/lys2Δ0 met15Δ0/met15Δ0 trp1Δ63/trp1Δ63 TLC1/tlc1Δ::LEU2* | This study |
| HKy668, 669 | CVy242 *RIF2/rif2Δ::kanMX4 RAP1/rap1::(RAP1-RIF2$_{60}$-URA3) TLC1/tlc1Δ::LEU2* | This study |
| JHUy912 | *MAT**a**/MATα his3Δ1/his3Δ1 leu2Δ0/leu2Δ0 lys2Δ0/lys2Δ0 met15Δ0/met15Δ0 trp1Δ63/trp1Δ63 ura3Δ0/ura3Δ0 XRS2/xrs2::xrs2ΔCt-13myc-kanMX6 RIF2/rif2Δ::LEU2* | This study |
| HKy688, 689 | JHUy912 *RAP1/rap1::(RAP1-RIF2$_{60}$-URA3)* | This study |

**Table S4: Primers used in the construction of *rif2 NAAIRS* mutants**

| ***rif2* mutant** | **Primer name** | **Sequence (5' to 3')** |
|---|---|---|
| WT | Rif2-up | CTGACATGGTTTTCATACAC |
| WT | Rif2-down | CAGCAACCAAATCCAAGTCCTAG |
| WT | Rif2-forward | ATATAGATATAAATACGAACGTGGTTAGTATATAGAGACACGGATCCCCGGGTTAATTAA |
| WT | Rif2-reverse | TCTTTGTATTGTTCGAACTCTTTCAAAAGACCTTGGTAATGAATTCGAGCTCGTTTAAAC |
| NAAIRS 2 | NAAIRS 2 reverse | CCTTATAGGTGCAAACGATCGTATAGCATCATTCATTGTCTCTATATA |
| | Anti-NAAIRS 2 forward | TATATAGAGACAATGAATGCTGCTATACGATCGTTTGCACCTATAAGG |
| NAAIRS 8 | NAAIRS 8 reverse | AACAACCTTTTTCGACGATCGTATAGCATCATTATCGGAATCTACATG |
| | Anti-NAAIRS 8 forward | CATGTAGATTCCGATAATGCTGCTATACGATCGTCGAAAAAGGTTGTT |
| NAAIRS 14 | NAAIRS 14 reverse | CACAATCTTGTCACTCGATCGTATAGCATCATTTCTCCTTATAGGTGC |
| | Anti-NAAIRS 14 forward | GCACCTATAAGGAGAAATGCTGCTATACGATCGAGTGACAAGATTGTG |
| NAAIRS 20 | NAAIRS 20 reverse | ATCATCGCTTATTGCCGATCGTATAGCATCATTGTCAACAACCTTTTT |
| | Anti-NAAIRS 20 forward | AAAAAGGTTGTTGACAATGCTGCTATACGATCGGCAATAAGCGATGAT |
| NAAIRS 26 | NAAIRS 26 reverse | AAAATTTTTTTGCTCCGATCGTATAGCATCATTTTTCACAATCTTGTC |
| | Anti-NAAIRS 26 forward | GACAAGATTGTGAAAAATGCTGCTATACGATCGGAGCAAAAAAATTTT |
| NAAIRS 32 | NAAIRS 32 reverse | CAACTTTCTCAGTACCGATCGTATAGCATCATTCAAATCATCGCTTAT |
| | Anti-NAAIRS 32 forward | ATAAGCGATGATTTGAATGCTGCTATACGATCGGTACTGAGAAAGTTG |
| NAAIRS 38 | NAAIRS 38 reverse | TTTAATTGGAACAAGCGATCGTATAGCATCATTAGTAAAATTTTTTTG |
| | Anti-NAAIRS 38 forward | CAAAAAAATTTTACTAATGCTGCTATACGATCGCTTGTTCCAATTAAA |
| NAAIRS 44 | NAAIRS 44 reverse | TGGGCTGCTAACACTCGATCGTATAGCATCATTGTTCAACTTTCTCAG |
| | Anti-NAAIRS 44 forward | CTGAGAAAGTTGAACAATGCTGCTATACGATCGAGTGTTAGCAGCCCA |
| NAAIRS 50 | NAAIRS 50 reverse | ACTCGGCTTACACACCGATCGTATAGCATCATTTTTTTTAATTGGAAC |
| | Anti-NAAIRS 50 forward | GTTCCAATTAAAAAAAATGCTGCTATACGATCGGTGTGTAAGCCGAGT |
| NAAIRS 56 | NAAIRS 56 reverse | CACTCGCTCCTTAACCGATCGTATAGCATCATTCTTTGGGCTGCTAAC |
| | Anti-NAAIRS 56 forward | GTTAGCAGCCCAAAGAATGCTGCTATACGATCGGTTAAGGAGCGAGTG |
| NAAIRS 62 | NAAIRS 62 reverse | CTGGTAGAAAACATGCGATCGTATAGCATCATTTGGACTCGGCTTACA |
| | Anti-NAAIRS 62 forward | TGTAAGCCGAGTCCAAATGCTGCTATACGATCGCATGTTTTCTACCAG |
| NAAIRS 68 | NAAIRS 68 reverse | GGCCATTGATTTGAACGATCGTATAGCATCATTGTCCACTCGCTCCTT |
| | Anti-NAAIRS 68 forward | AAGGAGCGAGTGGACAATGCTGCTATACGATCGTTCAAATCAATGGCC |
| NAAIRS 74 | NAAIRS 74 reverse | GGTGCCTAGCTCTTGCGATCGTATAGCATCATTCTTCTGGTAGAAAAC |
| | Anti-NAAIRS 47 forward | GTTTTCTACCAGAAGAATGCTGCTATACGATCGCAAGAGCTAGGCACC |
| NAAIRS 80 | NAAIRS 80 reverse | GCTTATTGACAAATACGATCGTATAGCATCATTCAAGGCCATTGATTT |
| | Anti-NAAIRS 80 forward | AAATCAATGGCCTTGAATGCTGCTATACGATCGTATTTGTCAATAAGC |
| NAAIRS 86 | NAAIRS 86 reverse | ACTTAAGCTCGGAACCGATCGTATAGCATCATTATTGGTGCCTAGCTC |
| | Anti-NAAIRS 86 forward | GAGCTAGGCACCAATAATGCTGCTATACGATCGGTTCCGAGCTTAAGT |
| NAAIRS 92 | NAAIRS 92 reverse | ATTTTTTGAAAGAAACGATCGTATAGCATCATTGTAGCTTATTGACAA |
| | Anti-NAAIRS 92 forward | TTGTCAATAAGCTACAATGCTGCTATACGATCGTTTCTTTCAAAAAAT |
| NAAIRS 98 | NAAIRS 98 reverse | ATTTTTCATACTCCTCGATCGTATAGCATCATTCTTACTTAAGCTCGG |
| | Anti-NAAIRS 98 forward | CCGAGCTTAAGTAAGAATGCTGCTATACGATCGAGGAGTATGAAAAAT |
| NAAIRS 104 | NAAIRS 104 reverse | GTCGAAGAAAACGATCGATCGTATAGCATCATTAAGATTTTTTGAAAG |
| | Anti-NAAIRS 104 forward | CTTTCAAAAAATCTTAATGCTGCTATACGATCGATCGTTTTCTTCGAC |
| NAAIRS 110 | NAAIRS 110 reverse | GTGTATATGTTCAACCGATCGTATAGCATCATTACAATTTTTCATACT |
| | Anti-NAAIRS 110 forward | AGTATGAAAAATTGTAATGCTGCTATACGATCGGTTGAACATATACAC |
| NAAIRS 116 | NAAIRS 116 reverse | GTCGATACCAGCATACGATCGTATAGCATCATTTTTGTCGAAGAAAAC |
| | Anti-NAAIRS 116 forward | GTTTTCTTCGACAAAAATGCTGCTATACGATCGTATGCTGGTATCGAC |
| NAAIRS 122 | NAAIRS 122 reverse | TGTTTCTGAAACTGCCGATCGTATAGCATCATTTTGGTGTATATGTTC |
| | Anti-NAAIRS 122 forward | GAACATATACACCAAAATGCTGCTATACGATCGGCAGTTTCAGAAACA |
| NAAIRS 128 | NAAIRS 128 reverse | TATATCGACTAAAGACGATCGTATAGCATCATTACGGTCGATACCAGC |
| | Anti-NAAIRS 128 forward | GCTGGTATCGACCGTAATGCTGCTATACGATCGTCTTTAGTCGATATA |
| NAAIRS 134 | NAAIRS 134 reverse | TTCTATAATTACGACCGATCGTATAGCATCATTCAGTGTTTCTGAAAC |
| | Anti-NAAIRS 134 forward | GTTTCAGAAACACTGAATGCTGCTATACGATCGGTCGTAATTATAGAA |
| NAAIRS 140 | NAAIRS 140 reverse | CATTAAGTAGTCATTCGATCGTATAGCATCATTATTTATATCGACTAA |
| | Anti-NAAIRS 140 forward | TTAGTCGATATAAATAATGCTGCTATACGATCGAATGACTACTTAATG |

**Table S4**, *continued*

| *rif2* mutant | Primer name | Sequence (5' to 3') |
|---|---|---|
| NAAIRS 146 | NAAIRS 146 reverse | TGATTGAATACCCTCCGATCGTATAGCATCATTCATTTCTATAATTAC |
| | Anti-NAAIRS 146 forward | GTAATTATAGAAATGAATGCTGCTATACGATCGGAGGGTATTCAATCA |
| NAAIRS 152 | NAAIRS 152 reverse | ACATTCTTTTGATTTCGATCGTATAGCATCATTTTTCATTAAGTAGTC |
| | Anti-NAAIRS 152 forward | GACTACTTAATGAAAAATGCTGCTATACGATCGAAATCAAAAGAATGT |
| NAAIRS 158 | NAAIRS 158 reverse | CTGCCCCATTGACTCCGATCGTATAGCATCATTGCTTGATTGAATACC |
| | Anti-NAAIRS 158 forward | GGTATTCAATCAAGCAATGCTGCTATACGATCGGAGTCAATGGGGCAG |
| NAAIRS 164 | NAAIRS 164 reverse | TTGTCCGCTATATGACGATCGTATAGCATCATTGATACATTCTTTTGA |
| | Anti-NAAIRS 164 forward | TCAAAAGAATGTATCAATGCTGCTATACGATCGTCATATAGCGGACAA |
| NAAIRS 170 | NAAIRS 170 reverse | ACTAGCTTCGAAATCCGATCGTATAGCATCATTAGCCTGCCCCATTGA |
| | Anti-NAAIRS 170 forward | TCAATGGGGCAGGCTAATGCTGCTATACGATCGGATTTCGAAGCTAGT |
| NAAIRS 176 | NAAIRS 176 reverse | GTGATTTGAAGGTTTCGATCGTATAGCATCATTTAGTTGTCCGCTATA |
| | Anti-NAAIRS 176 forward | TATAGCGGACAACTAAATGCTGCTATACGATCGAAACCTTCAAATCAC |
| NAAIRS 182 | NAAIRS 182 reverse | CATCATTAGGTCAGACGATCGTATAGCATCATTTTCACTAGCTTCGAA |
| | Anti-NAAIRS 182 forward | TTCGAAGCTAGTGAAAATGCTGCTATACGATCGTCTGACCTAATGATG |
| NAAIRS 188 | NAAIRS 188 reverse | TATTTTCCTCATAACCGATCGTATAGCATCATTCGTGTGATTTGAAGG |
| | Anti-NAAIRS 188 forward | CCTTCAAATCACACGAATGCTGCTATACGATCGGTTATGAGGAAAATA |
| NAAIRS 194 | NAAIRS 194 reverse | GATACTTTCGTCATTCGATCGTATAGCATCATTCATCATCATTAGGTC |
| | Anti-NAAIRS 194 forward | GACCTAATGATGATGAATGCTGCTATACGATCGAATGACGAAAGTATC |
| NAAIRS 200 | NAAIRS 200 reverse | GAAGTAGACAATATGCGATCGTATAGCATCATTATTTATTTTCCTCAT |
| | Anti-NAAIRS 200 forward | ATGAGGAAAATAAATAATGCTGCTATACGATCGCATATTGTCTACTTC |
| NAAIRS 206 | NAAIRS 206 reverse | ATCTAATTGTTCGAACGATCGTATAGCATCATTATCGATACTTTCGTC |
| | Anti-NAAIRS 206 forward | GACGAAAGTATCGATAATGCTGCTATACGATCGTTCGAACAATTAGAT |
| NAAIRS 212 | NAAIRS 212 reverse | AGTTGAAGTAGATAACGATCGTATAGCATCATTTTTGAAGTAGACAAT |
| | Anti-NAAIRS 212 forward | ATTGTCTACTTCAAAAATGCTGCTATACGATCGTTATCTACTTCAACT |
| NAAIRS 218 | NAAIRS 218 reverse | CTTCGAAGGTTCTATCGATCGTATAGCATCATTTTTATCTAATTGTTC |
| | Anti-NAAIRS 218 forward | GAACAATTAGATAAAAATGCTGCTATACGATCGATAGAACCTTCGAAG |
| NAAIRS 224 | NAAIRS 224 reverse | ATTGATAAATTCGGTCGATCGTATAGCATCATTTATAGTTGAAGTAGA |
| | Anti-NAAIRS 224 forward | TCTACTTCAACTATAAATGCTGCTATACGATCGACCGAATTTATCAAT |
| NAAIRS 230 | NAAIRS 230 reverse | TTCAAGTACCGATAACGATCGTATAGCATCATTAAGCTTCGAAGGTTC |
| | Anti-NAAIRS 230 forward | GAACCTTCGAAGCTTAATGCTGCTATACGATCGTTATCGGTACTTGAA |
| NAAIRS 236 | NAAIRS 236 reverse | TGCAATGTTATTACTCGATCGTATAGCATCATTAACATTGATAAATTC |
| | Anti-NAAIRS 236 forward | GAATTTATCAATGTTAATGCTGCTATACGATCGAGTAATAACATTGCA |
| NAAIRS 242 | NAAIRS 242 reverse | ATAAATGAGGACCTTCGATCGTATAGCATCATTTTTTTCAAGTACCGA |
| | Anti-NAAIRS 242 forward | TCGGTACTTGAAAAAAATGCTGCTATACGATCGAAGGTCCTCATTTAT |
| NAAIRS 248 | NAAIRS 248 reverse | AATGCTAACGTTATTCGATCGTATAGCATCATTAAATGCAATGTTATT |
| | Anti-NAAIRS 248 forward | AATAACATTGCATTTAATGCTGCTATACGATCGAATAACGTTAGCATT |
| NAAIRS 254 | NAAIRS 254 reverse | TGTCGATAGGAGAGACGATCGTATAGCATCATTTGAATAAATGAGGAC |
| | Anti-NAAIRS 254 forward | GTCCTCATTTATTCAAATGCTGCTATACGATCGTCTCTCCTATCGACA |
| NAAIRS 260 | NAAIRS 260 reverse | GAGTTTCTTTTTGAGCGATCGTATAGCATCATTCGAAATGCTAACGTT |
| | Anti-NAAIRS 260 forward | AACGTTAGCATTTCGAATGCTGCTATACGATCGCTCAAAAAGAAACTC |
| NAAIRS 266 | NAAIRS 266 reverse | CACAGTATATTTTGTCGATCGTATAGCATCATTGGATGTCGATAGGAG |
| | Anti-NAAIRS 266 forward | CTCCTATCGACATCCAATGCTGCTATACGATCGACAAAATATACTGTG |
| NAAIRS 272 | NAAIRS 272 reverse | TAATATCGGCATCTCCGATCGTATAGCATCATTGTTGAGTTTCTTTTT |
| | Anti-NAAIRS 272 forward | AAAAAGAAACTCAACAATGCTGCTATACGATCGGAGATGCCGATATTA |
| NAAIRS 278 | NAAIRS 278 reverse | TTGTTCTTGAGCGCACGATCGTATAGCATCATTAAACACAGTATATTT |
| | Anti-NAAIRS 278 forward | AAATATACTGTGTTTAATGCTGCTATACGATCGTGCGCTCAAGAACAA |
| NAAIRS 284 | NAAIRS 284 reverse | CATTTTTTTCAAATACGATCGTATAGCATCATTTGTTAATATCGGCAT |
| | Anti-NAAIRS 284 forward | ATGCCGATATTAACAAATGCTGCTATACGATCGTATTTGAAAAAAATG |
| NAAIRS 290 | NAAIRS 290 reverse | ATCAAAGGTAAACTTCGATCGTATAGCATCATTTTCTTGTTCTTGAGC |
| | Anti-NAAIRS 290 forward | GCTCAAGAACAAGAAAATGCTGCTATACGATCGAAGTTTACCTTTGAT |
| NAAIRS 296 | NAAIRS 296 reverse | TAATAACTTGCTTCCCGATCGTATAGCATCATTTATCATTTTTTTCAA |
| | Anti-NAAIRS 296 forward | TTGAAAAAAATGATAAATGCTGCTATACGATCGGGAAGCAAGTTATTA |
| NAAIRS 302 | NAAIRS 302 reverse | AAGCGAGTTGTAAGACGATCGTATAGCATCATTGGAATCAAAGGTAAA |
| | Anti-NAAIRS 302 forward | TTTACCTTTGATTCCAATGCTGCTATACGATCGTCTTACAACTCGCTT |

**Table S4**, *continued*

| *rif2* mutant | Primer name | Sequence (5' to 3') |
|---|---|---|
| NAAIRS 308 | NAAIRS 308 reverse | ATTCAACTGGCATGTCGATCGTATAGCATCATTCTGTAATAACTTGCT |
| | Anti-NAAIRS 308 forward | AGCAAGTTATTACAGAATGCTGCTATACGATCGACATGCCAGTTGAAT |
| NAAIRS 314 | NAAIRS 314 reverse | TAAGTTGGATTCTTTCGATCGTATAGCATCATTGACAAGCGAGTTGTA |
| | Anti-NAAIRS 314 forward | TACAACTCGCTTGTCAATGCTGCTATACGATCGAAAGAATCCAACTTA |
| NAAIRS 320 | NAAIRS 320 reverse | AAATTCGAAAAAGATCGATCGTATAGCATCATTATTATTCAACTGGCA |
| | Anti-NAAIRS 320 forward | TGCCAGTTGAATAATAATGCTGCTATACGATCGATCTTTTTCGAATTT |
| NAAIRS 326 | NAAIRS 326 reverse | GTGCGGAAAGACCTTCGATCGTATAGCATCATTTGCTAAGTTGGATTC |
| | Anti-NAAIRS 326 forward | GAATCCAACTTAGCAAATGCTGCTATACGATCGAAGGTCTTTCCGCAC |
| NAAIRS 332 | NAAIRS 332 reverse | AAACAAATAGGTAAACGATCGTATAGCATCATTCAAAAATTCGAAAAA |
| | Anti-NAAIRS 332 forward | TTTTTCGAATTTTTGAATGCTGCTATACGATCGTTTACCTATTTGTTT |
| NAAIRS 338 | NAAIRS 338 reverse | AATCTCAGTGTAAGCCGATCGTATAGCATCATTAGGGTGCGGAAAGAC |
| | Anti-NAAIRS 338 forward | GTCTTTCCGCACCCTAATGCTGCTATACGATCGGCTTACACTGAGATT |
| NAAIRS 344 | NAAIRS 344 reverse | AGTTCTACTCTGGACCGATCGTATAGCATCATTGTTAAACAAATAGGT |
| | Anti-NAAIRS 344 forward | ACCTATTTGTTTAACAATGCTGCTATACGATCGGTCCAGAGTAGAACT |
| NAAIRS 350 | NAAIRS 350 reverse | ATCCAACAATTCATCCGATCGTATAGCATCATTTATAATCTCAGTGTA |
| | Anti-NAAIRS 350 forward | TACACTGAGATTATAAATGCTGCTATACGATCGGATGAATTGTTGGAT |
| NAAIRS 356 | NAAIRS 356 reverse | CAGTCTGTTTCTGATCGATCGTATAGCATCATTAAAAGTTCTACTCTG |
| | Anti-NAAIRS 356 forward | CAGAGTAGAACTTTTAATGCTGCTATACGATCGATCAGAAACAGACTG |
| NAAIRS 362 | NAAIRS 362 reverse | TGGGTAATTTTTTATCGATCGTATAGCATCATTCTTATCCAACAATTC |
| | Anti-NAAIRS 362 forward | GAATTGTTGGATAAGAATGCTGCTATACGATCGATAAAAAATTACCCA |
| NAAIRS 368 | NAAIRS 368 reverse | AAAGTTATAAGCACTCGATCGTATAGCATCATTTGTCAGTCTGTTTCT |
| | Anti-NAAIRS 368 forward | AGAAACAGACTGACAAATGCTGCTATACGATCGAGTGCTTATAACTTT |
| NAAIRS 374 | NAAIRS 374 reverse | AAGACGCTGGTTTTTCGATCGTATAGCATCATTATGTGGGTAATTTTT |
| | Anti-NAAIRS 374 forward | AAAAATTACCCACATAATGCTGCTATACGATCGAAAAACCAGCGTCTT |
| NAAIRS 380 | NAAIRS 380 reverse | TCGAGTTAACTTAAGCGATCGTATAGCATCATTCTTAAAGTTATAAGC |
| | Anti-NAAIRS 380 forward | GCTTATAACTTTAAGAATGCTGCTATACGATCGCTTAAGTTAACTCGA |
| NAAIRS 386 | NAAIRS 386 reverse | TTATCTATCATGTACCGATCGTATAGCATCATTTGGAAGACGCTGGTT |
| | Anti-NAAIRS 386 forward | AACCAGCGTCTTCCAAATGCTGCTATACGATCGGTACATGATAGATAA |
| NAAIRS 392 | NAAIRS 392 reverse | TCAAAAGACCTTGGTTTACGATCGTATAGCAGCATTTTTTCGAGTTAACTT |
| | Anti-NAAIRS 392 forward | AAGTTAACTCGAAAAAATGCTGCTATACGATCGTAAACCAAGGTCTTTTGA |

**Table S5: Primers for epitope-tagged *rif2* mutants**

| Primer Name | Sequence (5' to 3') | Primer Description |
|---|---|---|
| Myc F | GCGTCTTCCACTTAAGTTAACTCGAAAAGTACATGATAGACGGATCCCCGGGTTAATTAA | Tagging of NAAIRS mutants |
| Myc R | CGGTGGCGGCCGCTCTAGAACTAGTGGATCCCCCGGGCTGGAATTCGAGCTCGTTTAAAC | |
| HK3 | TACCTTTGATTCCGGAAGCAAGTTATT | |
| HK4 | AGGCTTACCACCACCACCACCACCACCACCACCTCTATCATGTACTTTTCG | |
| HK5 | CATGATAGAGGTGGTGGTGGTGGTGGTGGTGGTGGTAAGCCTATCCCTAAC | |
| HK6 | GGTGGCGGCCGCTCTAGAACGTAGAATCGAGACCGAG | |
| HK7 | CTCGGTCTCGATTCTACGTTCTAGAGCGGCCGCCACCG | |
| HK9 | TGGCACGACAGGTTTCCCGACTGGAAA | |
| HK16 | CTAATCAAGTTTTTTGGGGTCGAGGTG | Used for inserting the V5 tag upstream of RIf2 via overlap extension method |
| HK17 | ACGGAGGTGGGGTACCCAATTCGCCCTA | |
| HK18 | TTGGGTACCCCACCTCCGTTGTCTCTA | |
| HK19 | TTCTGTACACCATTCGGCGTTCTGCTG | |
| HK20 | GCCGAATGGTGTACAGAAGGGATCTTC | |
| HK15 | GGTTCAACTTTCTCAGTACAGTAAAAT | |
| HK113 | CCAAAAATTTCAGCAGAACGCCGAATGGTGATCAATTGAATAAATTGGTAAACTTCAC | |
| HK114 | GATGGTTAAGAAGATCCCTTCTGTACATATCTGTAAGCGCAATGTTTTCTTCATTG | |
| HK65 | GCATGTAGATTCCGATGCCGCACCTATAAGGAGATC | Site-directed mutagenesis 5' primer for Rif2F8A |
| HK66 | GATCTCCTTATAGGTGCGGCATCGGAATCTACATGC | Site-directed mutagenesis 3' primer for Rif2F8A |
| HK67 | GAGCATGTAGATTCCGATTTTTTCCCTATAAGGAGATCGAAAAAG | Site-directed mutagenesis 5' primer for Rif2A9F |
| HK68 | CTTTTTCGATCTCCTTATAGGGAAAAAATCGGAATCTACATGCTC | Site-directed mutagenesis 3' primer for Rif2A9F |
| HK69 | GTAGATTCCGATTTTGCAGCCATAAGGAGATCGAAAAAG | Site-directed mutagenesis 5' primer for Rif2P10A |
| HK70 | CTTTTTCGATCTCCTTATGGCTGCAAAATCGGAATCTAC | Site-directed mutagenesis 3' primer for Rif2P10A |
| HK71 | GATTCCGATTTTGCACCTGCAAGGAGATCGAAAAAGG | Site-directed mutagenesis 5' primer for Rif2I11A |
| HK72 | CCTTTTTCGATCTCCTTGCAGGTGCAAAATCGGAATC | Site-directed mutagenesis 3' primer for Rif2I11A |
| HK73 | GATTCCGATTTTGCACCTATAGCGAGATCGAAAAAGGTTGTTG | Site-directed mutagenesis 5' primer for Rif2R12A |
| HK74 | CAACAACCTTTTTCGATCTCGCTATAGGTGCAAAATCGGAATC | Site-directed mutagenesis 3' primer for Rif2R12A |
| HK75 | GATTTTGCACCTATAAGGGCATCGAAAAAGGTTGTTG | Site-directed mutagenesis 5' primer for Rif2R13A |
| HK76 | CAACAACCTTTTTCGATGCCCTTATAGGTGCAAAATC | Site-directed mutagenesis 3' primer for Rif2R13A |
| HK77 | GATTTTGCACCTATAAGGAGAGCAAAAAAGGTTGTTGACAGTGAC | Site-directed mutagenesis 5' primer for Rif2S14A |
| HK78 | GTCACTGTCAACAACCTTTTTTGCTCTCCTTATAGGTGCAAAATC | Site-directed mutagenesis 3' primer for Rif2S14A |
| HK79 | CACCTATAAGGAGATCGGCAAAGGTTGTTGACAGTG | Site-directed mutagenesis 5' primer for Rif2K15A |
| HK80 | CACTGTCAACAACCTTTGCCGATCTCCTTATAGGTG | Site-directed mutagenesis 3' primer for Rif2K15A |
| HK81 | CTATAAGGAGATCGAAAGCGGTTGTTGACAGTGAC | Site-directed mutagenesis 5' primer for Rif2K16A |
| HK82 | GTCACTGTCAACAACCGCTTTCGATCTCCTTATAG | Site-directed mutagenesis 3' primer for Rif2K16A |
| HK83 | CTATAAGGAGATCGAAAAAGGCTGTTGACAGTGACAAGATTG | Site-directed mutagenesis 5' primer for Rif2V17A |

Table S5, *continued*

| Primer Name | Sequence (5' to 3') | Primer Description |
|---|---|---|
| HK84 | CAATCTTGTCACTGTCAACAGCCTTTTTCGATCTCCTTATAG | Site-directed mutagenesis 3' primer for Rif2V17A |
| HK85 | GGAGATCGAAAAAGGTTGCTGACAGTGACAAGATTGTG | Site-directed mutagenesis 5' primer for Rif2V18A |
| HK86 | CACAATCTTGTCACTGTCAGCAACCTTTTTCGATCTCC | Site-directed mutagenesis 3' primer for Rif2V18A |
| HK87 | GAGATCGAAAAAGGTTGTTGCTAGTGACAAGATTGTGAAAGC | Site-directed mutagenesis 5' primer for Rif2D19A |
| HK88 | GCTTTCACAATCTTGTCACTAGCAACAACCTTTTTCGATCTC | Site-directed mutagenesis 3' primer for Rif2D19A |
| HK21 | GTGAAAGCAATAGCCGATGATTTGGAG | Site-directed mutagenesis 5' primer for Rif2AA28 |
| HK22 | CTCCAAATCATCGGCTATTGCTTTCAC | Site-directed mutagenesis 3' primer for Rif2AA28 |
| HK33 | CAAAAAAATTTTACTGCCCTGAGAAAGTTGAACC | Site-directed mutagenesis 5' primer for Rif2V38A |
| HK34 | GGTTCAACTTTCTCAGGGCAGTAAAATTTTTTTG | Site-directed mutagenesis 3' primer for Rif2V38A |
| HK35 | GCAAAAAAATTTTACTGTAGCCAGAAAGTTGAACCTTGTTCC | Site-directed mutagenesis 5' primer for Rif2L39A |
| HK35 | GGAACAAGGTTCAACTTTCTGGCTACAGTAAAATTTTTTTGC | Site-directed mutagenesis 3' primer for Rif2L39A |
| HK37 | AAATTTTACTGTACTGGCAAAGTTGAACCTTGTTC | Site-directed mutagenesis 5' primer for Rif2R40A |
| HK38 | GAACAAGGTTCAACTTTGCCAGTACAGTAAAATTT | Site-directed mutagenesis 3' primer for Rif2R40A |
| HK39 | TTACTGTACTGAGAGCGTTGAACCTTGTTCC | Site-directed mutagenesis 5' primer for Rif2K41A |
| HK40 | GGAACAAGGTTCAACGCTCTCAGTACAGTAA | Site-directed mutagenesis 3' primer for Rif2K41A |
| HK41 | CTGTACTGAGAAAGGCGAACCTTGTTCCA | Site-directed mutagenesis 5' primer for Rif2L42A |
| HK42 | TGGAACAAGGTTCGCCTTTCTCAGTACAG | Site-directed mutagenesis 3' primer for Rif2L42A |
| HK43 | GTACTGAGAAAGTTGGCCCTTGTTCCAATTA | Site-directed mutagenesis 5' primer for Rif2N43A |
| HK44 | TAATTGGAACAAGGGCCAACTTTCTCAGTAC | Site-directed mutagenesis 3' primer for Rif2N43A |
| HK51 | GTACTGAGAAAGTTGAACGCCGTTCCAATTAAAAAAAG | Site-directed mutagenesis 5' primer for Rif2L44A |
| HK52 | CTTTTTTTAATTGGAACGGCGTTCAACTTTCTCAGTAC | Site-directed mutagenesis 3' primer for Rif2L44A |
| HK23 | GTTGÍAACATATACACCAAGCTGCTGGTATCGACCGTG | Site-directed mutagenesis 5' primer for Rif2AA122 |
| HK24 | CACGGTCGATACCAGCAGCTTGGTGTATATGTTCAAC | Site-directed mutagenesis 3' primer for Rif2AA122 |
| HK25 | CATATACACCAATATGCTGCTATCGACCGTGCAGTTTC | Site-directed mutagenesis 5' primer for Rif2AA124 |
| HK26 | GAAACTGCACGGTCGATAGCAGCATATTGGTGTATATG | Site-directed mutagenesis 3' primer for Rif2AA124 |
| HK27 | CATATACACCAATATGCTGGTGCCGACCGTGCAGTTTCAGAAAC | Site-directed mutagenesis 5' primer for Rif2AA125 |
| HK28 | GTTTCTGAAACTGCACGGTCGGCACCAGCATATTGGTGTATATG | Site-directed mutagenesis 3' primer for Rif2AA125 |
| HK29 | CCAATATGCTGGTATCGCCCGTGCAGTTTCAGAAAC | Site-directed mutagenesis 5' primer for Rif2AA126 |

Table S5, *continued*

| Primer Name | Sequence (5’ to 3’) | Primer Description |
|---|---|---|
| HK30 | GTTTCTGAAACTGCACGGGCGATACCAGCATATTGG | Site-directed mutagenesis 3' primer for Rif2AA126 |
| HK31 | CACCAATATGCTGGTATCGACGCTGCAGTTTCAGAAACACTGTC | Site-directed mutagenesis 5' primer for Rif2AA127 |
| HK32 | GACAGTGTTTCTGAAACTGCAGCGTCGATACCAGCATATTGGTG | Site-directed mutagenesis 3' primer for Rif2AA127 |
| HK53 | CTTCGAAGCTTACCGAATTTGCCAATGTTTTATCGGTACTTG | Site-directed mutagenesis 5' primer for Rif2I233A |
| HK54 | CAAGTACCGATAAAACATTGGCAAATTCGGTAAGCTTCGAAG | Site-directed mutagenesis 3' primer for Rif2I233A |
| HK55 | GAAGCTTACCGAATTTTGCAATGTTTTATCGGTAC | Site-directed mutagenesis 5' primer for RIf2I233C |
| HK56 | GTACCGATAAAACATTGCAAAATTCGGTAAGCTTC | Site-directed mutagenesis 3' primer for RIf2I233C |
| HK57 | GACAAAGTTGAACATATAGCCCAATATGCTGGTATCG | Site-directed mutagenesis 5' primer for RIf2H120A |
| HK58 | CGATACCAGCATATTGGGCTATATGTTCAACTTTGTC | Site-directed mutagenesis 3' primer for Rif2H120A |
| HK63 | GATCATATTGTCTACTTCAAATTCCAACAATTAGATAAATTATCTACTTC | Site-directed mutagenesis 5' primer for Rif2E213Q |
| HK64 | GAAGTAGATAATTTATCTAATTGTTGGAATTTGAAGTAGACAATATGATC | Site-directed mutagenesis 3' primer for Rif2E213Q |
| HK61 | CGACATCCCTCAAAAAGGCACTCAACACAAAATATAC | Site-directed mutagenesis 5' primer for Rif2K269A |
| HK62 | GTATATTTTGTGTTGAGTGCCTTTTTGAGGGATGTCG | Site-directed mutagenesis 3' primer for Rif2K269A |

**Table S6: Primers used in the construction of *RAP1-RIF2* fusions at the *RAP1* locus**

| Primer Name | Sequence (5' to 3') | Primer Description |
|---|---|---|
| HK89 | CGGGGGATCCACTAGTTCTAGAGCGGCCGCGATCTGAT GGTCTTTCCTCGCTATTTCTTG | Used to amplify the C-terminus of *RAP1*; to be used in the construction of the *RAP1-RIF2*$_{60}$ |
| HK90 | CCTCACTAAAGGGAACAAAAGCTGGAGCTCTGCTAATGG GATTCTATAAAACTGTTCCGC | |
| HK97 | GATTTTTTGAGAAGGACCTGTTAGGTGGCGGAGGTGGC GGAGGTGGCGGAGGTATGGAGCATGTAGATTCCG | |
| HK98 | CGGAATCTACATGCTCCATACCTCCGCCACCTCCGCCAC CTCCGCCACCTAACAGGTCCTTCTCAAAAAATC | |
| HK93 | GCAGCCCAAAGGTGTGTAAGCCGAGTTTATTCAATTCAA TTCATCATTTTTTTTTTATTC | |
| HK94 | GAATAAAAAAAAAATGATGAATTGAATTGAATAAACTCGG CTTACACACCTTTGGGCTGC | Used to construct the *URA* homology region for insertion of *RAP1-RIF2*$_{60}$ construct into yeast chromosome |
| HK95 | CATATTTGAGAAGATGCGGCCAGCAAAACTAAGTAATTG AATTAAGTAACATCATTGTTTAAC | |
| HK96 | GTTAAACAATGATGTTACTTAATTCAATTACTTAGTTTTGC TGGCCGCATCTTCTCAAATATG | |
| HK115 | ACAATGTTAATCCTCCTCCCAAC | Forward primer for lifting out *RAP1-RIF2*$_{60}$ |
| HK116 | GCGTGACATAACTAATTACATGAAGATCTCTAACTCGGCT TACACACCTTTG | Reverse primer for lifting out *RAP1-RIF2*$_{60}$ |
| HK117 | CAAAGGTGTGTAAGCCGAGTTAGAGATCTTCATGTAATTA GTTATGTCACGC | Forward primer for *CYC1* fragment |
| HK118 | GAATAAAAAAAAAATGATGAATTGAATTGCAAATTAAAGC CTTCGAGCGTC | Reverse primer for *CYC1* fragment |
| HK119 | GACGCTCGAAGGCTTTAATTTGCAATTCAATTCATCATTT TTTTTTTATTC | Forward primer for lifting out part of *URA3* promoter |
| HK120 | TGCAGGTTTTTGTTCTGTGCAGTTG | Reverse primer for lifting out part of *URA3* promoter |
| HK121 | TAGAGATCTTCATGTAATTAGTTATG | Forward primer for making *RAP1-RIF2*$_{36}$ construct from *RAP1-RIF2*$_{60}$ construct |
| HK123 | AAAATTTTTTTGCTCCAAATCATCGC | Reverse primer for making *RAP1-RIF2*$_{36}$ construct from *RAP1-RIF2*$_{60}$ construct |
| HK124 | GCATGTAGATTCCGATTATGCACCTATAAGGAGATC | Forward primer for making F8Y construct |
| HK125 | GATCTCCTTATAGGTGCATAATCGGAATCTACATGC | Reverse primer for making F8Y construct |
| HK126 | CATGTAGATTCCGATTGGGCACCTATAAGGAGAT | Forward primer for making F8W construct |
| HK127 | GATCTCCTTATAGGTGCCCAATCGGAATCTACATG | Reverse primer for making F8W construct |
| HK128 | CGGGGGATCCACTAGTTCTAGAGCGGCCGCGATTGCAC GAGAATTTTTCAAGCATTTTGC | Forward primer for making *rap1*$\Delta$*C* fragment |
| HK129 | ACCTCCGCCACCTCCGCCACCTCCGCCACCGGGCAAAC TATTTGAAATATTGGATAGATC | Reverse primer for making *rap1*$\Delta$*C* fragment in fusion |
| HK130 | GATCTATCCAATATTTCAAATAGTTTGCCCGGTGGCGGA GGTGGCGGAGGTGGCGGAGGT | Forward primer for making *RIF2* fragment for *rap1*$\Delta$*C* Gibson |
| HK131 | CCTTTTCGGTTAGAGCGGATGTGGGAGGAGGGC | Reverse primer for making *RIF2* fragment for *rap1*$\Delta$*C* Gibson |
| HK132 | GCGTGACATAACTAATTACATGAAGATCTCTAGGGCAAA CTATTTGAAATATTGGATAG | Reverse primer for making *rap1*$\Delta$*C* plasmid (forward primer is HK128) |
| HK133 | GCGGTCAAGAAGCAGTTTTA | Forward primer for confirming *rap1*$\Delta$*C* construct at *RAP1* locus |
| OCC85 | ATTGCCATTGCAAAATCGTTTTTGTGGTCAATTTGCAATG AGATTGTACTGAGAGTGCAC | Deletion of *RIF1* |
| OCC86 | ATTTATTGCCATTTTGATCTATTCTACATACTAACAATCAC TGTGCGGTATTTCACACCG | Deletion of *RIF1* |
| OCC122 | TAGATATAAATACGAACGTGGTTAGTATATAGAGACAATG AGATTGTACTGAGAGTGCAC | Deletion of *RIF2* |
| OCC123 | TTGTATTGTTCGAACTCTTTCAAAAGACCTTGGTAATTTA CTGTGCGGTATTTCACACCG | Deletion of *RIF2* |
| OCC168 | GGTTCTGGTGGCATCTAT | Deletion of *TLC1* |
| OCC171 | ATGCTTGCCGGAAAGCTG | Deletion of *TLC1* |
| Yprime FWD | CGCGAATTCGCCCTACAGCACTTCTACATAGC | Y' fragment for Southern analysis |
| Yprime REV | CGAGAATTCCAGCGTTTGCGTTCCATGACG | Y' fragment for Southern analysis |